REPUBLIC OF TURKEY

ADANA ALPARSLAN TÜRKEŞ SCIENCE AND TECHNOLOGY UNIVERSITY

GRADUATE SCHOOL OF NATURAL AND APPLIED SCIENCES

DEPARTMENT OF BIOENGINEERING

DOUBLE-IMPRINTED POLYMERS FOR SELECTIVE HSA DEPLETION FROM HUMAN SERUM

OKAN ZENGER

MASTER OF SCIENCE

ADANA, 2021

REPUBLIC OF TURKEY

ADANA ALPARSLAN TÜRKEŞ SCIENCE AND TECHNOLOGY UNIVERSITY

GRADUATE SCHOOL OF NATURAL AND APPLIED SCIENCES

DEPARTMENT OF BIOENGINEERING

DOUBLE-IMPRINTED POLYMERS FOR SELECTIVE HSA DEPLETION FROM HUMAN SERUM

OKAN ZENGER

MASTER OF SCIENCE

SUPERVISOR

ASSOC. PROF. GÖZDE BAYDEMİR PEŞİNT

ADANA, 2021

ETHICS

I hereby declare that all information in this thesis has been obtained and presented in accordance with academic rules, all audio-visual and written information and results have been presented according to the rules of scientific ethics, all cited studies have been fully referenced. There is not any distortion in the data set, and results fully reflect the reality. Any part of this thesis has not been presented as another thesis study.

[Signature]

Okan ZENGER

ABSTRACT

DOUBLE-IMPRINTED POLYMERS FOR SELECTIVE HSA DEPLETION FROM HUMAN SERUM

Okan ZENGER

Department of Bioengineering

Supervisor: Assoc. Prof. Gözde BAYDEMİR PEŞİNT

January 2021, 69 pages

Human Serum Albumin (HSA) is the most abundant protein in human blood plasma−it constitutes about half of serum proteins. As in the all proteomic studies of the blood plasma, high-abundant proteins, i.e. albumin, hemoglobin, interfere with the analysis of low-abundant and disease-related proteins, so removal or depletion of these proteins is vital for proteomic studies. In this thesis study, it was aimed to deplete HSA from human serum in one step using double-imprinted cryogels, prior to use in proteomic analysis. For this purpose, HSA-imprinted cryogels were synthesized with 8% monomer concentration and a second imprinting step with 16% monomer concentration in presence of HSA was achieved on the first gel. Thereby, HSA double-imprinted cryogel columns (HSA-DIP) were obtained. Cryogel column synthesized by double-layer imprinting technique but not containing template molecule (DL-NIP) and monolayer HSA-specific polymers with monomer concentrations of 8% and 16% (called HSA-$MIP_{8\%}$ and HSA-$MIP_{16\%}$, respectively) were synthesized as the control group. Synthesized columns were characterized by swelling tests, Scanning Electron Microscopy (SEM), mercury porosimetry and Micro Computed Tomography (Micro-CT) analysis. The water uptake ratios were calculated as 84% for HSA-DIP, 82% for DL-NIP, 89% for HSA-$MIP_{8\%}$ and 88% for HSA-$MIP_{16\%}$. Surface areas of HSA-DIP, DL-NIP, HSA-$MIP_{16\%}$ and HSA-$MIP_{8\%}$ were found to be 39 m^2/g, 37m^2/g, 21 m^2/g and 12 m^2/g, respectively. HSA adsorption capacity was investigated, and selectivity studies were performed against Human Hemoglobin (Hb) and Immunoglobulin G (IgG) molecules which occupy a significant portion of human serum. Obtaining results were investigated by kinetic analyses to determine adsorption properties of the system. Finally, depletion of HSA directly from human serum was studied. In addition, HSA-DIP columns were tested in terms of reusability, and it was

demonstrated that they can be used up to 10 times without significant decrease in selective HSA adsorption capacity.

Keywords: high-abundant proteins, Human Serum Albumin, depletion, molecular imprinting technology, cryogels, double-imprinted polymers, enhanced adsorption capacity.

ÖZET

ÇİFT-TABAKALI BASKILANMIŞ KRİYOJELLER: İNSAN SERUMUNDAN HSA MOLEKÜLÜNÜN UZAKLAŞTIRILMASI

Okan ZENGER

Biyomühendislik

Danışman: Doç. Dr. Gözde BAYDEMİR PEŞİNT

Ocak 2021, 69 Sayfa

İnsan Serum Albümini (HSA) insan kanında en bol bulunan serum proteinidir, serum proteinlerinin yaklaşık yarısını oluşturur. Kan plazmasının proteomik çalışmalarında, albümin ve hemoglobin gibi kanda bol miktarda bulunan proteinler, düşük miktarda bulunan ve hastalıkların teşhisi ile ilgili olabilecek proteinlerin analizini zorlaştırmaktadır. Bu yüzden, bu proteinlerin uzaklaştırılması veya azaltılması proteomik çalışmalar için hayati öneme sahiptir. Bu tez çalışmasında, çift-tabakalı baskılanmış kriyojeller kullanılarak HSA'nın direkt olarak insan serumundan tek adımda azaltılması amaçlanmıştır. Çalışma kapsamında, ilk olarak HSA-baskılanmış kriyojeller %8 monomer konsantrasyonu ile sentezlenmiştir. Daha sonra, %8'lik kriyojel üzerine HSA içeren %16'lık polimer çözeltisi dökülerek, ilk kriyojel tabakasının birbirleriyle bağlantılı makrogözenekleri arasında ikinci polimer çözeltisinin jelleşmesi sağlanmıştır. Böylelikle, HSA-baskılanmış çift tabakalı polimerler (HSA-DIP) elde edilmiştir. Kontrol grubu olarak, çift-tabakalı baskılama tekniği ile üretilmiş fakat kalıp molekül içermeyen polimerler (DL-NIP) ve farklı monomer konsantrasyonlarında üretilmiş tek tabakalı HSA-spesifik polimerler (%8 ve %16 monomer konsantrasyonu için sırasıyla; HSA-$MIP_{8\%}$ ve HSA-$MIP_{16\%}$) sentezlenmiş ve elde edilen sonuçlar birbirleriyle karşılaştırılmıştır. Sentezlenen kriyojel kolonları şişme testleri, Taramalı Elektron Mikroskobu (SEM), cıva porozimetresi ve Mikro Bilgisayarlı Tomografi (Mikro-CT) analizi ile karakterize edilmiştir. Şişme oranları HSA-DIP için %84, DL-NIP için %82, HSA-$MIP_{8\%}$ için %89 ve HSA-$MIP_{16\%}$ için %88 olarak hesaplandı. HSA-DIP, DL-NIP, HSA-$MIP_{16\%}$ ve HSA-$MIP_{8\%}$ kriyojel kolonların yüzey alanları sırasıyla 39 m^2/g, 37 m^2/g, 21 m^2/g ve 12 m^2/g olarak bulundu. Sonrasında, HSA tanıma bölgeleriyle ilişkili olarak HSA'nın sulu çözeltilerden adsorpsiyonu incelenmiştir. Ayrıca, HSA-DIP kolonlarının HSA molekülü için seçiciliği İnsan Hemoglobin (Hb) ve İmmünoglobulin G (IgG) yarışmacı moleküllerine karşı test

edilmiştir. Elde edilen sonuçlar, sistemin adsorpsiyon özelliklerini belirlemek için kinetik analizlerle incelenmiştir. Son olarak, doğrudan insan serumundan HSA'nın azaltılması incelenmiştir. Ayrıca, çift-tabakalı baskılanmış polimerler yeniden kullanılabilirlik çalışmaları ile test edilmiş ve 10 adsorpsiyon-desorpsiyon döngüsünden sonra bile HSA-DIP kolonlarının HSA adsorpsiyon kapasitelerini önemli ölçüde koruduğu sonucuna ulaşılmıştır.

Anahtar Kelimeler: İnsan Serum Albümini, moleküler baskılama teknolojisi, kriyojeller, çift-tabakalı baskılanmış polimerler, artırılmış adsorpsiyon kapasitesi.

Dedicated to Assoc. Prof. Gözde Baydemir Peşint who has become a role model in my both academic career and daily life, with all the help and encouragement when I was trying to figure out who I am, by seeing and bringing out the potential hidden inside of me,

...and to my beloved family who has always been there for me, not only to celebrate my achievements, but also to make up for my youth mistakes.

ACKNOWLEDGEMENTS

Performing my MSc thesis study was an incredible experience and it wouldn't be possible to complete it without all the support and encouragement of my supervisor, colleagues, friends and family.

First, I would like to thank my dear supervisor, Assoc. Prof. Gözde Baydemir Peşint, for her valuable guidance, professional advice, constructive criticism and suggestions during my research, as well as her sincere interest and efforts to be always there for me in need, like a family. I am having a hard time here finding a sentence to express my gratitude to her, but I know she will be understanding about it as she always does.

Special thanks to Dr. Sibel Özdaş and Dr. Hatice İmge Oktay Başeğmez, not only because of their guiding suggestions during my study, but also enabling us to work in a warm and cheerful environment.

I would like to thank my friends, Burcu Eren, Bürge Ataözü, Büşra Kızılcık, Ece Kaya, Gizem Ece Derici, İpek Canatar, Mehtap Yıldırım, Mustafa Nergiz, Pırıl Arısoy (alphabetically arranged without any priorities), for their help and friendship, providing me a pleasant atmosphere to work in. We worked together, and we laughed together.

Thanks to all academic staff in Bioengineering, for their good intentions and understanding, and for making things easier during this process which is the first step of my academic career.

Special thanks to my brothers Muhittin Ünal and Anıl Esen for their friendship and all the assistance when I have a lot more work than the remaining time. When you work together, impossibilities become not only possible but also much easier.

I do not really think there is an appropriate word for you to feel how deeply grateful I am, for all the support and encouragement of my beloved family who has faith in me and has always been there for me, not only to celebrate my achievements but also to make up for my mistakes.

This thesis was financially supported by ATU BAP Coordination Unit with project number of 19103014.

TABLE OF CONTENTS

LIST OF FIGURES

LIST OF TABLES

NOMENCLATURE

µL	: Microliter
µm	: Micrometre
mL	: Milliliter
mg	: Microgram
cm	: Centimetre
L	: Liter
sec	: Second
min	: Minute
h	: Hour
eq.	: Equation
M	: Molarity
°C	: Celsius degree
MIP	: Molecularly Imprinted Polymer
NaCl	: Sodium Chloride
Ultrapure water	: UW
PBS	: Phosphate - buffered saline
TEMED	: N, N, N, N - Tetramethylethylenediamine
APS	: Ammonium persulfate
VIM	: 4-Vinylimidazole
HEMA	: 2-Hydroxyethylmethacrylate
P(HEMA)	: Poly(2-Hydroxyethylmethacrylate)
MBAA	: N, N'-Methylenebisacrylamide
HSA	: Human Serum Albumin
Hb	: Human Hemoglobin
IgG	: Immunoglobulin G
SDS-PAGE	: Sodium Dodecyl Sulfate Polyacrylamide Gel Electrophoresis
UV	: Ultraviolet

1. INTRODUCTION

Human bodily fluids, e.g. blood, urine and saliva, are complex matrices consisting of many elements such as ions, lipids, sugars, proteins, etc (Hu et al., 2006). Blood consists of blood cells and plasma and circulates through the body. Blood is a significant biological fluid which contains substances e.g. oxygen, glucose, etc., required by cells and transports them all around the body as one of the main parts of the circulatory system. More than half of the total blood consists of plasma, which is the liquid part with a water content of about 90%. Serum differs from plasma in that serum is devoid of clotting agents, i.e. fibrinogen. Serum is mostly used for blood typing but is also used for diagnostic testing (Hu et al., 2006; Mathew et al., 2020). Plasma, on the other hand, is mostly used for blood-clotting related problems (Hu et al., 2006).

Human serum is a key bodily fluid which contains a quantity of proteins which serve as biomarkers for the determination of a wide variety of diseases including diabetes, cancer types, cardiovascular diseases and neurodegenerative diseases as well as any infection or inflammation (Jacobs et al., 2005, Hu et al., 2006). Human serum has a key role in diagnosis, prognosis and monitoring of physiological circumstances. Accordingly, the determination of serum proteins provides a significant knowledge in the early diagnosis of diseases (Braun et al., 2000; Hu et al., 2006; Mattiasson et al., 2009; Schirhagl et al., 2010; Chen et al., 2011; Gao et al., 2013; Koutroukides et al., 2013; Suwinski et al., 2019).

Human serum consists of more than one million different proteins and approximately 99% of the total serum contains high-abundant proteins such as albumin, immunoglobulin (A and G), antitrypsin and transferrin. Among these, Human Serum Albumin (HSA) which is synthesized by liver, makes up half of high-abundant proteins in human serum (Lindsey, 1996; Fanali et al., 2012). HSA is a monomeric multi-domain macromolecule which is predominantly arranged in the α-helix held together by 17 disulfide bridges and has a molecular weight of about 67 kDa (Hülshoff et al., 2013). The outside of its structure is like a cylinder and is polar, while the middle part is nonpolar and allows the hydrophobic substrates to be bonded (Wang et al., 2013; Guizado, 2014; Merlot et al., 2014). In healthy individuals, the reference HSA concentration varies between 3.5-5.0 g/dL (McCallum et al., 2014; Ma et al., 2017; Huang et al., 2017; Guo et al., 2018; Singh et al., 2018). HSA molecule exhibits an extraordinary ligand binding capacity

and is an important carrier protein for many endogenous and exogenous compounds such as neutral and weak acidic metabolites, fatty acids and steroids, etc. (Heli et al., 2007; Merlot et al., 2014).

Detection, purification, quantification, depletion and removal of biomacromolecules are of great importance in several areas, including immunodiagnostics and biotechnology (Zhang et al., 2013). Due to the complexity of human serum, proteomic analysis of serum is a challenging process which requires the initial removal or depletion of high-abundant proteins. Complex structure of human serum can be easily eliminated by removing high amounts of proteins, minimizing their masking effect on low-abundant proteins, which might be significant biomarkers in diagnosis and prognosis of diseases, and follow-up of treatment (Bereli et al., 2010; Schalich et al., 2020). It has become a vital demand to use inexpensive and highly effective techniques to remove large amounts of proteins in human serum, which take up a lot of space and cast a shadow upon low-abundant but important proteins. Therefore, depletion high-abundant proteins especially HSA is generally the first step in serum- and plasma-based proteomics analysis where the detection and quantification of low-abundant proteins is the primary purpose (Bereli et al., 2010; Garcia-Martinez et al., 2015; Jesus et al., 2017; Schalich et al., 2020).

Recently, separation of proteins is carried out by various chromatographic methods, selective adsorption and soft gel applications (Tamahkar et al., 2011). Molecular imprinting is a modern technique used for the synthesis of polymers with specific binding sites for the template molecule by polymerization of monomers in the presence of the template molecule (Tamahkar et al., 2011; Chen et al., 2011; Resmini, 2012; Sharma et al.,2012; Kartal and Denizli, 2014; Baydemir and Denizli, 2015). In molecular imprinting technique, the target molecule is used as the template during the synthesis of the polymeric system, to create specific cavities for the attachment of the desired molecule. Recognition and specific adsorption properties of the molecularly imprinted polymers (MIPs) depend on the physical and geometrical characteristics including size, shape and overall charge, as well as the chemical properties of the template (Alexander et al., 2006; Kartal and Denizli, 2014; Baydemir and Denizli, 2015). Molecular imprinting technique mainly encompass the following three steps:

1. Preparation of pre-complex which consists of the template molecule and a convenient ligand;

2. Polymerization of monomers around the pre-complex;
3. Removal of template molecule from the polymeric system to generate specific adsorption cavities for the desired molecule (Tamahkar et al., 2011; Kartal and Denizli, 2014; Baydemir and Denizli, 2015).

MIPs have come to the forefront among other materials used for removal or depletion of high-abundant proteins in human serum, due to ease of preparation, relatively high selective adsorption capacity toward molecule of interest, mechanical strength and stability under harsh conditions. One of the most significant features of MIPs is that they can be used several times without any remarkable decrease in adsorption capacity of the material, since MIPs are able to maintain stability of their structure under physically harsh environments (Ciardelli et al., 2006; Alexander et al., 2006). They are cheaper to produce in large scale with relatively higher yield, as compared to other affinity techniques (Ye et al., 1999; Say et al., 2003; Andac et al., 2004; Daniel et al., 2005; Ersoz et al., 2005; Yavuz et al., 2005; Pang and Cheng, 2006; Haginaka, 2008).

MIPs have been the focus of research because of their excellent molecular recognition properties and are of great interest for applications requiring the binding and separation of specific molecular species. Mechanical and chemical stability of these polymers have made them extremely important in many fields ranging from chromatography to assays, sensor technology, catalysis and controlled release systems (Ye et al., 1999; Say et al., 2003; Andac et al., 2004; Daniel et al., 2005; Ersoz et al., 2005; Yavuz et al., 2005; Pang and Cheng, 2006; Haginaka, 2008). Until now, low molecular weight compounds, polypeptides, proteins, viral particles and even bacteria have been used as template molecules in molecular imprinting technology (Hoshino et al., 2008; Mengfan et al., 2018; Piletsky et al., 2020).

Cryogels are affinity matrices synthesized at minus temperatures via cryotropic polymerization process and owing to their spongy and supermacroporous morphology, which allows to work with viscous fluids with particles, e.g. milk and blood, without clogging the column (Lozinsky et al., 2003; Noppe et al., 2007; Baydemir and Denizli, 2015). Cryogels draw attention by their relatively reduced flow resistance, shorter diffusion distance, etc. features for both adsorption and desorption processes (Dainiak et al., 2007; Kumar and Srivastava, 2010). Cryogels have many application areas due to their osmotic, chemical and mechanical stability; they are

commonly used in molecular imprinting technology. However, adsorption capacity of cryogels for proteins is low due to the interconnected supermacropores within the matrix (i.e., low surface area) and flexibility of three-dimensional structures of proteins. Improving the binding capacity of supermacroporous cryogels has a great importance in a bioseparation process (Dainiak et al., 2007; Kumar and Srivastava, 2010).

Several factors have been reported to affect surface morphology and average pore sizes of cryogels, including monomer concentration, solvent, synthesis temperature, presence of additives (e.g. sodium and calcium salts, and inhibitors), cooling rate which depends on the concentration of initiator and type of cooling (i.e. liquid cooling or air cooling) (Okay and Lozinsky, 2014). Despite the fact that the structure of the cryogels is not primarily affected by monomer concentration, it was demonstrated that approximate pore sizes are closely related to monomer concentration; increasing monomer concentration results in a significant decrease in pore sizes, when other parameters (synthesis conditions, cooling rate, type and volume of solvent, etc.) are kept constant (Özmen and Okay, 2005; Okay and Lozinsky, 2014; Bat, 2016).

In double-layer imprinting approach, a monolayer cryogel is synthesized with lower monomer concentration in presence of template molecule, and then second imprinting process was performed using a polymeric solution with higher monomer concentration in the supermacroporous structure of the first cryogel layer under certain conditions, increasing the specific surface area, so the adsorption capacity. Therefore, the synthesis of affinity systems with relatively large surface areas and much more cavities specific to the molecule of interest can be achieved (Mosbach and Ramström, 1996; Ye et al., 1999; Say et al., 2003; Andac et al., 2004; Ersöz et al., 2004; Daniel et al., 2005).

In this thesis study, it was aimed to synthesize a new generation of polymeric system, which provide a specific depletion of HSA directly from human serum in one step, with relatively enhanced binding capacities due to a significant increase in specific surface area, employing a fairly new approach and an innovative methodology: double-layer imprinting technique. Within the scope of the thesis study, synthesized adsorbents were evaluated in terms of morphology, adsorption properties, selectivity against competitor molecules, Hb and IgG, which occupy a significant portion of human serum, and reusability. Obtaining results were

investigated by adsorption isotherm models and kinetic analyses to determine adsorption behaviour of the system.

2. LITERATURE REVIEW

2.1. High-Abundant Proteins in Human Blood

Blood consists of blood cells and plasma, and circulates through the body. Blood is a significant biological fluid which contains substances e.g. oxygen, glucose, etc., required by cells and transports them all around the body as one of the main parts of the circulatory system. More than half of the total blood consists of plasma, which is the liquid part with a water content of about 90%. Serum differs from plasma in that serum is devoid of clotting agents, i.e. fibrinogen. Serum is mostly used for blood typing but is also used for diagnostic testing (Hu et al., 2006; Mathew et al., 2020). Plasma, on the other hand, is mostly used for blood-clotting related problems (see Figure 2.1) (Hu et al., 2006).

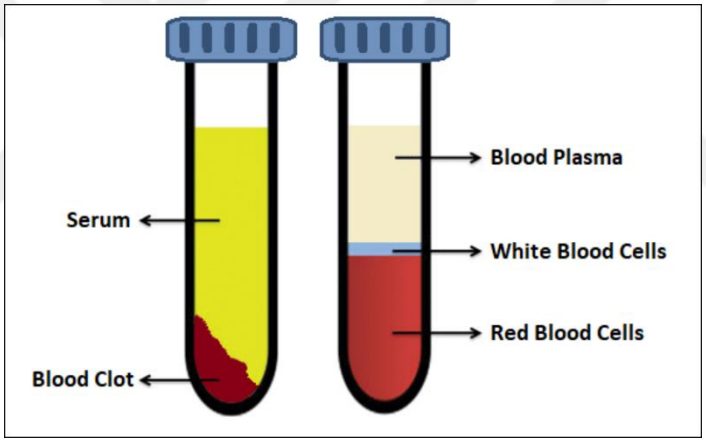

Figure 2.1. Serum and Plasma. Illustration of the discrimination of blood serum and plasma.

Human serum is a key bodily fluid which contains a quantity of proteins, which serve as biomarkers for the determination of a wide variety of diseases including diabetes, malnutrition, cancer types, cardiovascular diseases and neurodegenerative diseases as well as any infection or inflammation (Jacobs et al., 2005, Hu et al., 2006). Human serum has a key role in diagnosis, prognosis and monitoring of physiological circumstances. Accordingly, the determination and characterization of serum proteins provides a significant knowledge in the early diagnosis of diseases (Braun et al., 2000; Hu et al., 2006; Mattiasson et al., 2009; Schirhagl et al., 2010; Chen et al., 2011; Gao et al., 2013; Koutroukides et al., 2013; Suwinski et al., 2019).

Human serum consists of more than one million different proteins and and peptides in a large dynamic concentration (i.e., 60-80 mg/mL), approximately 99% of the total serum contains high-abundant proteins such as albumin, immunoglobulin (A and G), antitrypsin and transferrin (Lindsey, 1996; Fanali et al., 2012). In addition to the great contribution of human serum to proteomic studies, high-abundant serum proteins make proteomic analysis difficult, interfering with the analysis of extremely low-abundant proteins such as the vasoconstrictor peptide endothelin-1 (Schirhagl et al., 2010; Reichelt et al., 2014).

A significant contributing effect to the analytical challenge of serum proteome is that a single protein, i.e., albumin, makes up half of high-abundant proteins in human serum. Only 1% of the entire protein content of serum is made up of low-abundant proteins which are of great importance in proteomic studies in search of potential biomarkers in a wide variety of health conditions. Therefore, analysis of serum proteome should be started with an effort to decrease serum complexity by removal or depletion of one or more high-abundant protein(s), reducing their masking effect on low-abundant biomarkers (Hu et al., 2006; Schirhagl et al., 2010; Andaç, 2013; Asliyuce et al., 2013; Gökay et al., 2015).

A novel technique, which is relatively cost-effective and highly efficient as compared to available techniques for removal or depletion of high-abundant proteins in serum is still desirable. Other than well-known ultracentrifugal filtration technique, the most commonly used techniques for depletion of albumin from human serum are dye-affinity depletion (Cibacron Blue F3GA and its derivatives as ligand), immuno-affinity depletion (specific antibodies as ligand), immobilized metal affinity chromatography (IMAC), and molecular imprinting (see Table 2.1) (Tuncel et al., 1993; Denizli et al., 1997; Garipcan and Denizli, 2002; Govorukhina et al., 2003; Hu et al., 2006; Schirhagl et al., 2010; Tamahkar et al., 2010; Bereli et al., 2010; Andaç et al., 2012a; Andaç et al., 2013; Gun'ko et al., 2013; Hajizadeh et al., 2013; Uzun et al., 2013; Andaç, 2015).

Dye-affinity techniques, as compared to immune-affinity depletion, have been preferred due to their relatively low costs, high capacity and ease of preparation, however, were insufficient in terms of specificity (Odabaşı and Denizli, 2004; Ma et al., 2005; Hu et al., 2006; Altıntaş et al., 2007; Andaç et al., 2012a; Andaç et al., 2013; Asliyuce et al., 2013; Andaç, 2015; Gökay et al., 2015; de Jesus et al., 2017). Molecular Imprinting Technology (MIT) has come into prominence

among other techniques used for removal or depletion of high-abundant proteins in human serum, due to ease of preparation, relatively high selective adsorption capacity toward molecule of interest, mechanical strength and stability under harsh conditions (see Table 2.1) (Yao et al., 2007; Andaç et al., 2012b; Andaç et al., 2013).

Table 2.1. Protein Depletion. Commonly used methods used for the depletion of high-abundant proteins.

Classification	Methods	Properties
Affinity-based	Cibacron Blue dye	Low cost, high loading capacity, low specificity
	Peptide ligands	Low cost, high reproducibility, reactivity across species, low specificity
	Protein A/G	High affinity for immunoglobulins but not all subtypes
Size-based	Centrifugal ultrafiltration	Traditional method, low cost, low effectiveness, low reproducibility, lack of specificity
Antibody-based	Monoclonal antibody	High specificity, high cost, fail to remove the related fragment of the protein of interest
	IgG	Single-step depletion of multiple proteins, high affinity and high specificity, high cost, low sample capacity.

2.2. Historical and Clinical Perspective on Albumin

Albumin is one of the oldest known proteins and probably the most frequently studied protein which is the most abundant soluble protein in the body of all vertebrates (Peters, 1995; Hassan et al., 1997). Albumin has been the center of attention in the scientific world due to wide variety of functions. Since the time of Hippocrates, physiological properties of albumin have been partially characterized. Albumin was named and first studied in the late 1800s and crystallized at the beginning of the last century (Majoor, 1978). In ancient times when time-consuming and laborious methods were required for the purification of other proteins, the fact that high amounts of pure albumin could be obtained made albumin an important model protein for scientists. Albumin is also a genetically advantageous protein; genetic variations of albumin are very rare and generally harmless, while mutations in other proteins can result in some disorders or even be fatal (Hassan et al., 1997; Minchiotti et al., 2008). Albumin has many application

areas, especially clinical medicine and basic research. Changes in serum albumin concentration in the disease, typically malnutrition, kidney and liver disease, have long been used for diagnosis and prognosis (Hassan et al., 1997). Albumin, which is easily rendered virus-free by heating at 60 °C for 10 hours, is widely used in surgery and in the treatment of burns, hemorrhagic shock and trauma via infusion, due to potential viral contamination of blood and plasma, especially hepatitis and AIDS (Garcia-Martinez et al., 2015).

Serum albumin is a type of globular protein found in vertebrate blood. Bovine Serum Albumin (BSA) and Human Serum Albumin (HSA) are well known and most studied types of albumin (Steinhardt et al., 1971; Gelamo et al., 2002). BSA and HSA have high similarity in terms of structure and function (Steinhardt et al., 1971; Hawkins and Dugaiczyk, 1982; Gelamo et al., 2002).

HSA, which is synthesized by liver about 10-12 g each day, makes up half of high-abundant proteins in human serum (Lindsey, 1996; Caironi and Gattinoni, 2009; Fanali et al., 2012; Lee and Wu, 2015). HSA is a monomeric multi-domain macromolecule which is predominantly arranged in the α-helix held together by 17 disulfide bridges and has a molecular weight of about 67 kDa (see Figure 2.2) (Hülshoff et al., 2013). The outside of its structure is like a cylinder and is polar, while the middle part is nonpolar and allows the hydrophobic substrates to be bonded (Wang et al., 2013; Guizado, 2014; Merlot et al., 2014). HSA molecule exhibits an extraordinary ligand binding capacity and is an important carrier protein for many endogenous and exogenous compounds such as neutral and weak acidic metabolites, fatty acids and steroids, etc (Heli et al., 2007; Merlot et al., 2014). In healthy individuals, the reference HSA concentration varies between 3.5-5.0 g/dL (McCallum et al., 2014; Ma et al., 2017; Huang et al., 2017; Guo et al., 2018; Singh et al., 2018). HSA is the main protein that controls oncotic pressure and serves as the transporter of multiple endogenous as well as exogenous substances (e.g., drugs) throughout the body (Wang et al., 2013; Guizado, 2014; Merlot et al., 2014).

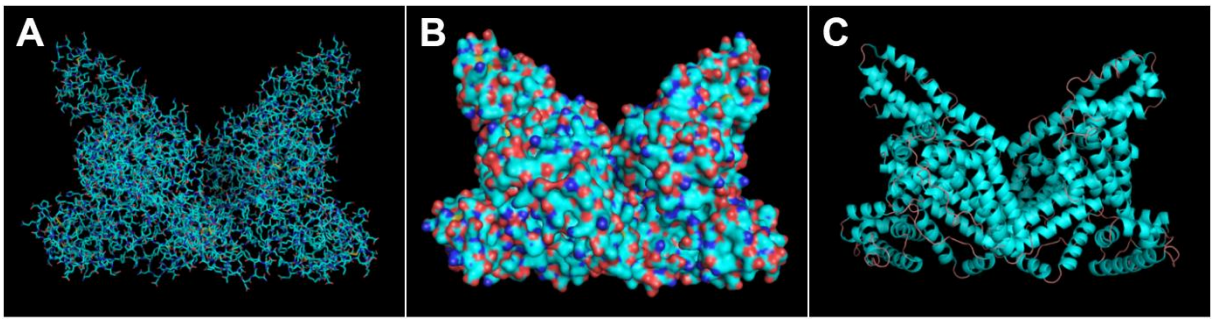

Figure 2.2. Molecular Structure of HSA. A) stick; B) space-filling; C) backbone and ribbon model of HSA (PDB ID: 1AO6, Sugio et al., 1999).

2.3. Molecular Imprinting Technology

2.3.1. Molecular Recognition and Molecular Imprinting Concepts

Molecular imprinting is a promising and rapidly developing technology (Verheyen et al., 2011). Molecular imprinting technology (MIT) is a remarkable synthetic approach to mimic natural molecular recognition (Ramström and Ansell, 1998; Alexander et al., 2006). Molecular recognition occurs when two molecules are complement to each other both chemically and geometrically, i.e. when two molecules are linked to each other by non-covalent bonds such as hydrogen bonds, electrostatic interactions, hydrophobic interactions, poor metal coordination, or when they fit together spatially in terms of size and shape (Ramström and Ansell, 1998; Tsukagoshi, 2001; Bergmann and Peppas, 2008; Hillberg and Tabrizian, 2008).

Molecular recognition is a ubiquitous phenomenon in nature, for example, binding of an enzyme to a substrate, entry of a virus into the cell through a receptor, recognition of antigen/antibody in the immune system, a drug to a biological target, formation of messenger RNA from DNA template molecules, binding of odor molecules to olfactory receptors found in nasal cavity, interactions between elements of neuronal signal transduction process. Therefore, molecular recognition can be considered as a driving force in all life processes (Tsukagoshi, 2001; Bergmann and Peppas, 2008; Hillberg and Tabrizian, 2008).

When there are molecules similar to a target molecule in the environment, selective recognition of the target molecule is required for biological and chemical processes. Molecularly imprinted polymers have advantages such as high physical strength, resistance to high temperature and pressure, stability against acids, bases, metal ions and organic solvents, low cost and easy

preparation, while MIPs prepared by conventional methods have low efficiency mass transfer in some applications, it has a number of disadvantages, such as the weak zones that the molecule can reach and the heterogeneous distribution of the binding sites. In addition, most polymerization systems are not compatible with water. An ideal solution for these problems is the development of molecular surface printing technique with sol-gel method (Tsukagoshi, 2001; Tan and Tong, 2007; Hu, 2013).

2.3.2. Synthesis of Molecularly Imprinted Polymers

MIT is based on the formation of selective recognition cavities in the structure of polymer with the memory of a template molecule, so that the polymeric material called "molecularly imprinted polymer (MIP)", can specifically bind to the molecule of interest (Alexander et al., 2006; Chen et al., 2011). These gaps are formed around the target molecule by polymerization of the cross-linker and functional monomer. The target molecule is removed from the resulting polymer (Alexander et al., 2006; Singabraya, 2012) and the binding sites are complementary to the target molecule in size, shape and placement of functional groups (see Figure 2.3).

MIT mainly encompass the following three steps:

1. Preparation of pre-complex which consists of the target molecule (template) and a convenient ligand (functional monomer);
2. Polymerization of cross-linkers and main monomers around the pre-complex;
3. Removal of template molecule from the polymeric system to generate specific adsorption cavities complementary to the template molecule in size, shape and placement of functional groups.

Thus, a molecular recognition memory is imprinted in the structure of polymeric material that can selectively reconnect the template molecule (Andersson, 2000; Alexander et al., 2006; Martín-Esteban, 2013).

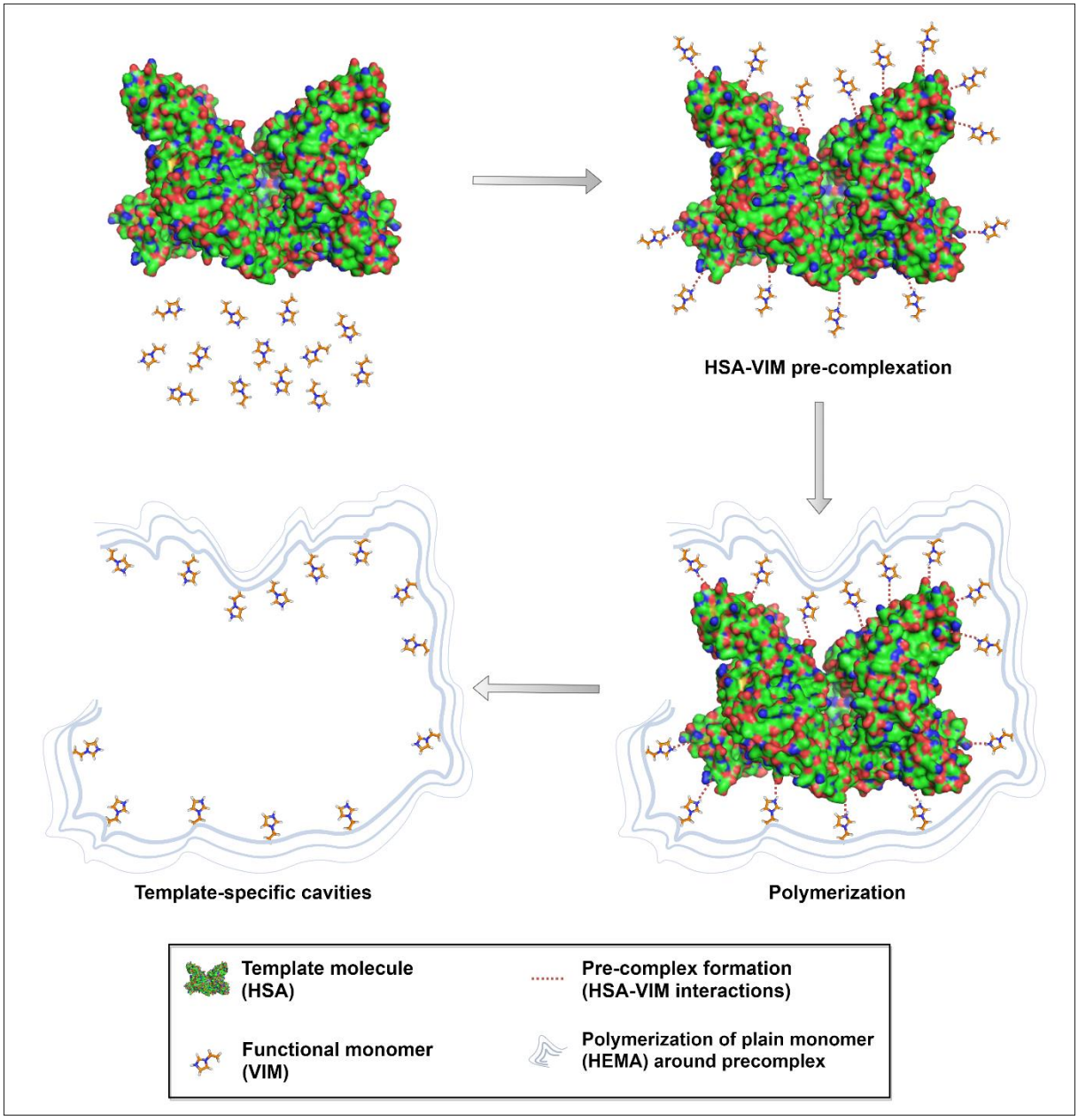

Figure 2.3. Molecular Imprinting Process. Representative illustration of molecular imprinting technique: pre-complexation, polymerization around pre-complex, removal of the template molecule and formation of template-specific cavities.

Compared to other recognition systems, MIPs have highlighted properties such as cost-effectiveness, ease of preparation, high stability and reusability under harsh chemical and physical conditions, MIPs have become increasingly attractive in many areas, especially in selective solid-phase extraction, chromatographic separation and chemical sensors (Alexander et al., 2006; Chen et al., 2011). MIPs can be synthesized basically with three different

approaches: non-covalent imprinting, covalent imprinting (see Figure 2.4) and semi-covalent imprinting.

2.3.2.1. Non-Covalent Imprinting

Non-covalent imprinting is the most commonly used procedure since it is relatively simple in practice. During the synthesis process, a suitable monomer or monomers are mixed together with the template molecule in a suitable porogen (solvent). After synthesis, the template molecule is simply removed from the polymer by washing the polymeric material with a solution which can easily eliminate non-covalent interactions and where the template molecule can be readily dissolved, without any alteration in the structure of polymer. Subsequently, reattachment (or adsorption) of the template molecule with MIP occurs via non-covalent interactions, such as ionic, hydrophobic and hydrogen bonds (Arshady and Mosbach, 1981; Hansen, 2007). The hydrogen bond is often employed as the molecular recognition interaction of MIPs. In this respect, acrylic acid and methacrylic acid are generally considered functional monomers since the carboxyl group functions simultaneously as a hydrogen donor and a hydrogen acceptor. Non-covalent interactions are easily eliminated by treatment with aqueous solutions of acids and bases or alcohol. Thus, template molecules can be removed from the polymeric network after polymerization. The non-covalent imprinting approach allows easy preparation of polymer, fast and reversible binding of the template molecule, and application of the technique to a wide variety of templates (Arshady and Mosbach, 1981; Yan and Row, 2006).

In this approach, binding of template to functional monomers is controlled thermodynamically, thus inadequate and non-specific binding sites may occur. Variable strengths of non-covalent interactions result in heterogeneous binding sites which reduce the rebinding activity (see Figure 2.4A) (Arshady and Mosbach, 1981; Alexander et al., 2006).

2.3.2.2. Covalent Imprinting

It takes place by the formation of covalent bonds between the template molecule and the functional monomer before the polymerization process. After synthesis, covalent bonds are broken to remove the template molecule from the polymer matrix (Wulff and Sarhan, 1972; Hansen, 2007). In this method, boronic acid esters, ketals, disulfide bonds, acetals and schiff bases are used as monomers (Bergmann and Peppas, 2008). In the covalent imprinting method,

the high stability of covalent bonds provides a more homogeneous distribution of the binding sites. The template molecule suitable for covalent imprinted is limited since the formation of identical recombinant sites requires rapid and reversible covalent bonds between the functional monomer and the template molecule. In addition, due to the strong covalent bonds, slow binding and dissociation make it difficult to reach thermodynamic equilibrium (Wulff and Sarhan, 1972; Hansen, 2007). In this approach, binding of template to functional monomers is controlled kinetically, which decreases the rate of template rebinding upon re-occupation of the cavities. The combination of preparation technique and template size/shape may give rise to diffusion problems and thus reduce in rebinding activity (see Figure 2.4B) (Alexander et al., 2006).

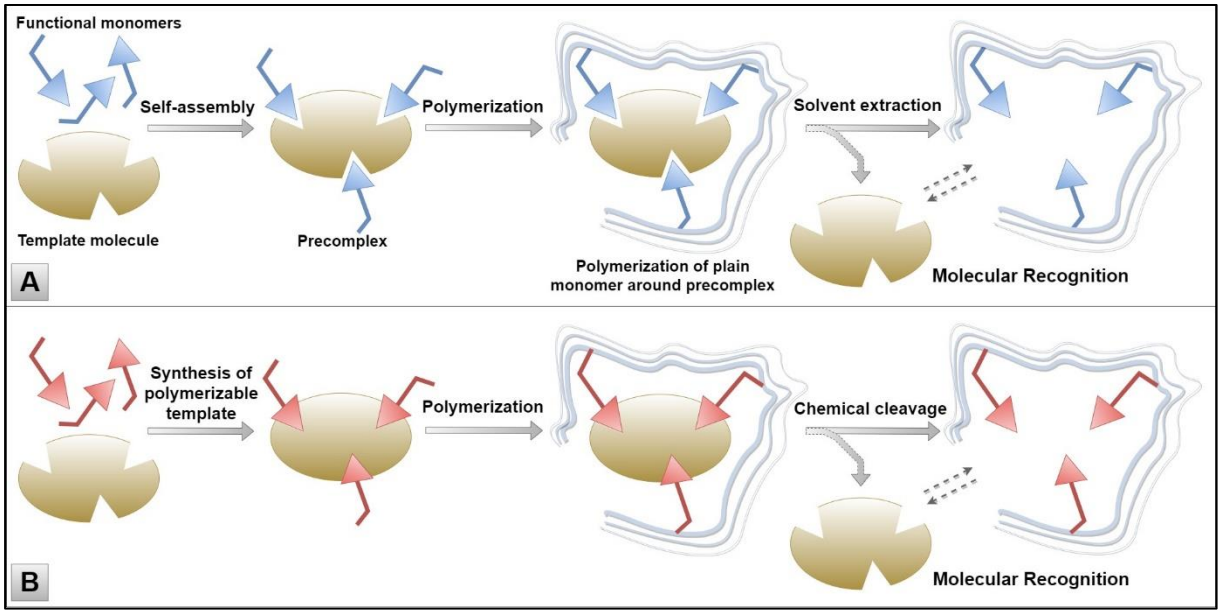

Figure 2.4. Molecular Imprinting Approaches. Schematic representation of A) non-covalent, and B) covalent molecular imprinting procedures.

2.3.2.3. Semi-Covalent Imprinting

It has emerged by combining covalent and non-covalent imprinting methods. In this approach, covalent bond is formed between the template molecule and the functional monomers before polymerization, after the template molecule is removed from the polymer matrix, reattachment of the analyte to the MIP occurs through non-covalent interactions as in the non-covalent suppression protocol (Hansen, 2007). The semi-covalent approach offers advantages such as the formation of homogeneous binding sites by covalent imprinting and rapid and reversible adsorption by non-covalent imprinting (Tan and Tong, 2007).

2.3.3. Synthesis Conditions

The polymerization reaction is primarily affected by several factors, including the polymerization temperature, time, volume of the polymeric solution, solvent (porogen), magnetic field, etc. as well as the concentration and type of the main components of the polymerization, i.e. template molecule, monomer, cross-linker and initiator, and size of the template molecule. Optimization of the reaction condition must be performed to obtain an ideal polymer, depending on the purpose of use (Alexander et al., 2006).

The selection of convenient ingredients is one of the most crucial steps in the molecular imprinting process. The template molecule, functional monomers, cross-linkers, initiators and solvent (porogen) are required for the preparation of molecularly imprinted polymers, and the amount of each determines the structure of the polymer, such as the pore size (Wullf, 1995; Yan and Row, 2006; Biçen, 2009; Çetin, 2013; Öncel, 2013; Çorman, 2014; Narula et al., 2014; Ersoy, 2018).

2.3.3.1. Template Molecule

In the vast majority of analytical processes, template molecules are target compounds. Any inorganic or organic molecules and biomacromolecules can be used as template molecules (target molecule) in molecular imprinting. An ideal template molecule should be free of functional groups which would interfere with the polymerization reaction, which can result in insufficient polymerization. Chemical stability and conformational integrity of a given template molecule are of great importance in the molecular imprinting process. Since template molecules with low chemical stability may change both chemically and geometrically in harsh reaction conditions, the molecular imprinting process may not result as intended. Limited success can be achieved in such imprinting of proteins due to major problems such as the highly flexible conformation of the proteins, the complexity of their surface structures, and the diversity of protein sequences. Such a polymerization process gives a rise to formation of non-specific binding cavities which the template molecule cannot bind or fit in (Dainiak et al., 2007; Chen et al., 2011; Fu et al., 2015; Jia et al., 2018).

Size of a molecule of interest is a significant factor to be taken into consideration. In MIT, imprinting of large templates, such as large proteins, virus particles and even bacterial cells, is a challenging process. Large structures of biological macromolecules cause restriction of

movement within the cross-linked polymer network and a decrease in the efficiency of reattachment and the conditions and reagents, and therefore, the reaction conditions must be modified according to the nature of the template (Dainiak et al., 2007; Chen et al., 2011; Ertürk and Mattiasson, 2017).

2.3.3.2. Monomers

The role of the monomer is provided by functional groups that can form a complex with the template molecule through covalent or non-covalent interactions (Shamsipur et al., 2007; Koohpaei et al., 2008; Zhang et al., 2008). The strength of the interactions between the template molecule and the monomer affects the affinity of MIPs and the selectivity of the recognition sites (Zhang et al., 2008). A stronger interaction results in a more stable complex and a higher binding capacity of the MIPs. Therefore, the correct selection of functional monomers is very important. The selection of a suitable monomer is usually made through challenging trial and error testing. Various strategies such as spectroscopic measurements (nuclear magnetic resonance, UV-vis, Fourier transform infrared spectroscopy, etc.), computer simulation and isothermal titration calorimetry have been used to select the most suitable functional monomer that can form a more stable complex to the template molecule (Vasapollo et al., 2011; Zink et al., 2018).

Methacrylic acid (MAA), glycidylmethacrylate (GMA), acrylic acid (AA), 2- or 4 vinylpyridine (2- or 4-VP), acrylamide, trifluoromethacrylic acid (TFM) and 2-hydroxyethylmethacrylate (HEMA) are widely used as monomers in MIT. The structures of various monomers are shown in Figure 2.5 (Vasapollo et al., 2011; Zink et al., 2018).

Generally, during the synthesis step, the molar ratio between monomer and template molecule affects the imprinting efficiency and affinity of MIPs. Low molar ratios create fewer binding sites in the polymer due to the smaller amount of the template-monomer complex, but although relatively high molar ratios create more non-specific binding capacity, binding selectivity decreases. Therefore, the molar ratio of the die to monomer must be optimized to achieve high efficiency printing efficiency. Functional monomers must contain compatible functional groups to combine with the template molecule (Yan and Row, 2006; Vasopollo et al., 2011; Çetin, 2013).

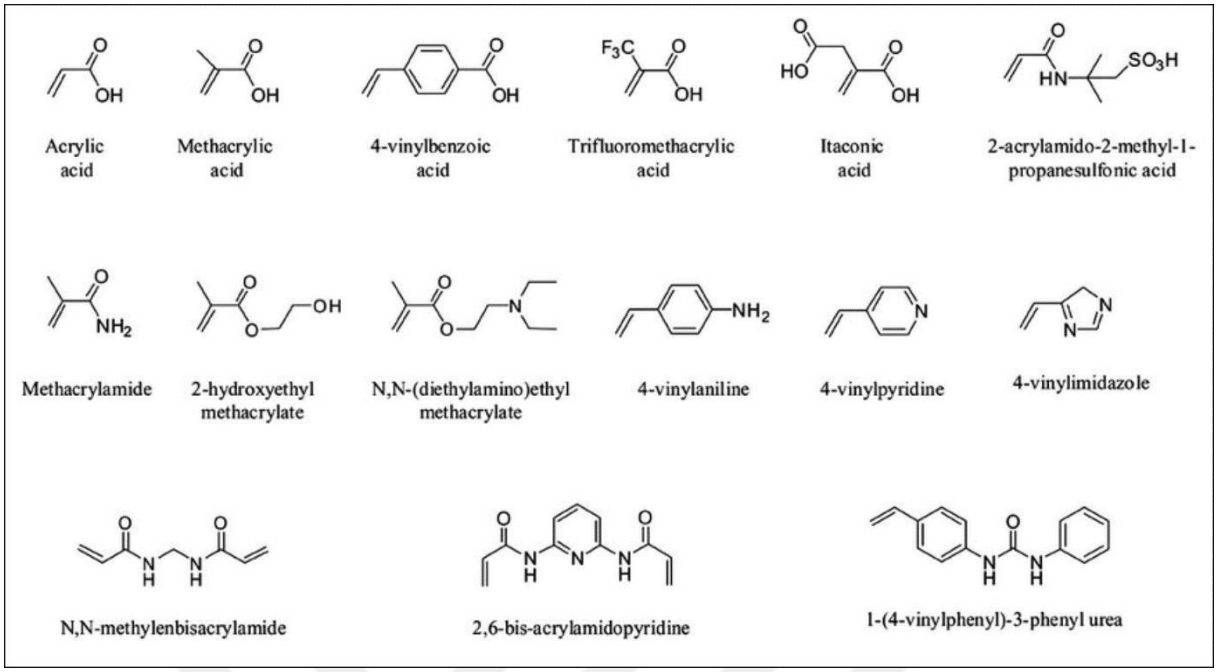

Figure 2.5. Functional Monomers. Commonly used functional monomers in molecular imprinting (Moreno-Bondi et al., 2008).

2.3.3.3. Cross-linker

Cross-linker acts as a bridge between functional groups of monomers, thus leading to the formation of a highly cross-linked polymeric material around imprinted molecules. Selective binding properties and binding capacity of a given polymer is highly affected by the type and concentration of cross-linker. Cross-linker concentration lower than enough results in insufficient cross-linking so that MIPs will be devoid of stability gap configurations. However, use of relatively higher concentration of cross-linkers will decrease the number of specific binding sites per unit of mass of MIPs due to the occurrence of non-covalent interactions and further heterogeneous copolymerization (Alexander et al., 2006).

There are a wide variety of cross-linkers employed in MIT studies including ethylene glycol methacrylate (EGDMA), trimethylolpropane trimethacrylate (TRIM), N,N-methylenebisacrylamide (MBAA), divinylbenzene (DVB) and pentaerythritol triacrylate (PETA). Molecular structures of the most widely used molecules as cross-linker are given in Figure 2.6. Cross-linkers are of great importance in molecular imprinting since these molecules maintain the conformational stability of recognition cavities and morphology of MIP. It can be said that a cross-linker serves as the skeleton in the structure of polymeric material (Alexander et al., 2006).

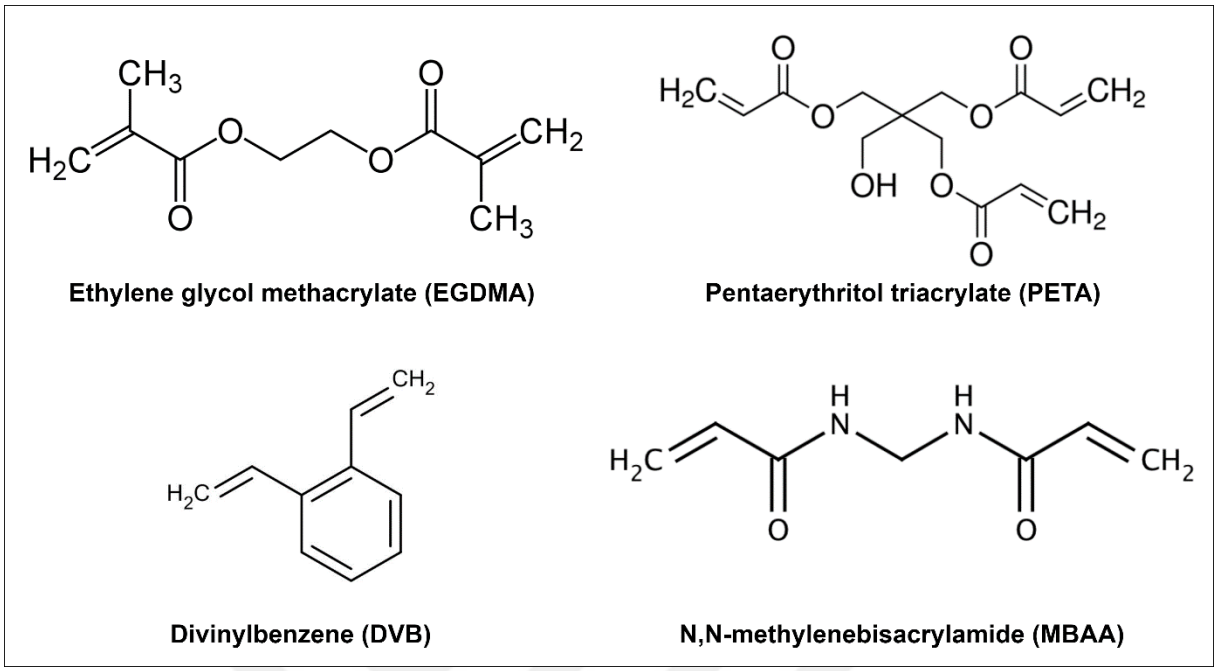

Figure 2.6. Cross-linkers. Commonly used cross-linkers in molecular imprinting (Moreno-Bondi et al., 2008).

2.3.3.4. Solvent

Solvent of the polymeric solution is employed as a porogen (or pore maker) during the synthesis of MIPs and is crucial in the polymerization process. Structure and size of micro- and macropores, morphology, swelling capability, mechanical strength and binding properties of polymer, as well as the imprinting process, are immensely affected by the solvent in the non-covalent interaction system. When all other components are kept constant, the amount of solvent in a polymeric system is an important parameter and should be optimized according to the size of the template molecule. Less than the required amount of solvent, thus higher monomer concentration than needed, generally results in harder and more intense structure with relatively smaller pore sizes, negatively affecting the imprinting process and obstructing both template removal and rebinding processes. The solvent also has a role to adjust the reaction temperature (Alexander et al., 2006; Yan and Row, 2006; Biçen, 2009; Vasopollo et al., 2011).

Aprotic and low polar organic solvents such as toluene, acetonitrile and chloroform are often used in non-covalent polymerization processes to ensure excellent imprinting efficiency. Furthermore, the recent approach where ultrapure water (UW) is used as the porogen, has drawn attention due to biocompatibility of MIPs (Chen et al., 2011).

2.3.3.5. Initiator/Catalyst System

Polymerization reactions require a starting force, called initiator/catalyst system which induces free radical formation, to initiate free radical polymerization. Some of the well-known and widely used initiators are benzoyl peroxidase, lauryl peroxidase, ammonium peroxidase, etc., which can be used either alone or mostly together with a catalyst, N,N,N',N'-tetramethylenediamine (TEMED). Initiator/catalyst system provides a fast polymerization. Polymerization process starts in seconds, after the initiator/catalyst system is added into a monomer solution (Alexander et al., 2006).

2.3.4. Cryogels

Cryogels are commonly used polymeric structure in MIT and are of great importance in biotechnology. Cryogels were first reported in the 1960s and their biotechnological and clinical importance was newly discovered (Lozinsky et al., 2003). Etymology of "cryogel" term is based on the Greek word "kryos" which means freezing or ice. Cryogelation (or gelation at temperatures below zero) allows the formation of macroporous cryogels whose porosity can be controlled (Lozinsky et al., 2003). Cryogels are three-dimensional gel matrices with macroporous or supermacroporous and spongy morphology. Their macroporous structure allow the mass transfer of various sizes to be carried out easily both by diffusion and convection.

Cryogels have gained importance in biological applications due to their osmotic, chemical and mechanical stability, so that, it has in many application areas. They have been used in the chromatography of biological nanoparticles (plasmids, viruses, cell organelles) (Njayou and Quash, 1991; Ardvisson et al., 2003) or immobilization of biopolymers (Kokufuta and Jinbo, 1992; Kumakura, 2001) or cells (Scardi, 1987). In addition, cryogels show rapid swelling kinetics due to their macroporous structure. They are commonly used in the design of biosensors and drug release systems (Lozinsky and Plieva, 1998; Plieva et al., 2005).

Recently, cryogels have also been used in molecular imprinting techniques. Cryogels can be formed by physical or chemical crosslinking of polymer networks. The polymer morphology obtained by cryotropic gelation is quite different from non-frozen systems (see Figure 2.7). Cryogels can be produced as cylinders, granules or discs according to their intended use (Lozinsky and Plieva, 1998; Plieva et al., 2005).

The interconnected macroporous and spongy morphology are typical of cryogels. Most of the water content of spongy cryogels is inside the macroporous structure and can be mechanically removed from the macropores by squeezing. The properties of the cryogels vary with the cryogelation temperature, the time in frozen state, the freezing/thawing rate, the type of solvent and the soluble or insoluble additives (Lozinsky and Plieva, 1998; Plieva et al., 2005).

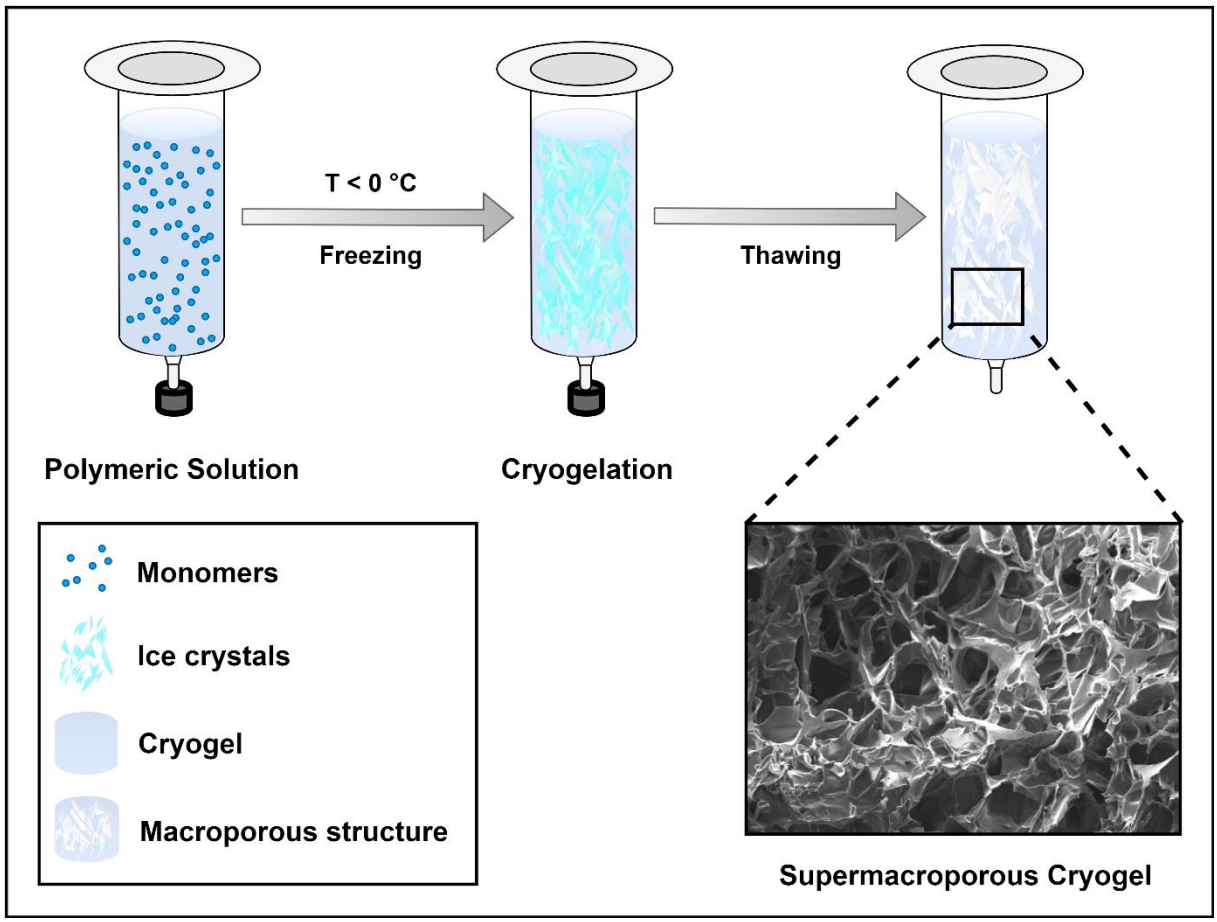

Figure 2.7. Cryogelation Process. Illustrative representation of supermacroporous cryogel synthesis.

Recently, molecularly imprinted polymers have been synthesized in the form of cryogel. The difference of cryogels from other gels is summarized below:

1. Cryogels can be formed by covalent, ionic or non-covalent bonds.
2. Cryogels can be synthesized in the form of blocks, granules, cylinders, tubes and discs.
3. Cryogels have interconnected three dimensional supermacroporous structures.
4. It is relatively cheap to produce and use for long periods (Lozinsky and Plieva, 1998; Plieva et al., 2005).

Morphological advantages of cryogels make it possible to study with viscous or heavy fluids with particles, such as milk and blood without blocking the column (Noppe et al., 2007; Lozinsky et al., 2003; Baydemir and Denizli, 2015). Cryogels draw attention by their relatively reduced flow resistance, shorter diffusion distance, etc. features for both adsorption and desorption processes (Dainiak et al., 2007; Kumar and Srivastava, 2010). However, the adsorption capacity of the cryogels for proteins is low due to the interconnected supermacropores within the matrix (i.e., low surface area). Improving the binding capacity of supermacroporous cryogels has a great importance in a bioseparation process (Dainiak et al., 2007; Kumar and Srivastava, 2010).

2.4. HSA-Imprinted Polymer Based Applications

Lin et al. (2004) prepared the MIPQCM sensor that can precisely determine the HSA concentration by imprinting HSA using 3-dimethylaminopropylmethacrylamide-acrylate. They applied the sensor prepared by coating the gold electrode of the QCM with HSA MIP to the clinical samples. The selectivity of the prepared material for HSA was tested against cytochrome C, myoglobin and lysozyme molecules and it was reported that MIPQCM sensors can adsorb HSA with high sensitivity, although these molecules have much smaller molecular weight than HSA (Lin et al., 2004).

Garipcan et al. (2004) studied HSA adsorption from aqueous solutions by synthesizing poly (hydroxyethyl methacrylate methacryloamidocysteine [poly- (HEMA-MAC)] beads. They found that the maximum adsorption capacity of Cu^{2+} chelated beads for HSA (193 mg/g) was much higher than the adsorption capacity of [poly-(HEMA-MAC)] beads (37 mg/g). It has been reported that Cu^{2+} chelation significantly increased HSA adsorption, however, the selectivity of the material for HSA, against competitive molecules, has not been tested within the scope of the study (Garipcan et al., 2004).

In the study of Bonini et al. (2007), the synthesis of poly-aminophenylboronic acid (ABPA) imprinted beads for the recognition of the protein HSA is reported. The binding capacity of synthesized beads for HSA was found to be 1.4 mg/g. The MIP beads were used for the first time as a tool for the pre-fractionation of the sample prior to proteome analysis, removal of the 58% of albumin in serum was achieved (Bonini et al., 2007).

Ghasemzadeh et al. (2008) synthesized artificial gel antibodies to determine the concentration of albumin in clinical samples easily and quickly using molecular imprinting technique and used it for quantitative analysis of albumin in cerebrospinai liquid (CSF) and human plasma. They have shown that this technique determines the albumin in these body fluids with high precision (Ghasemzadeh et al., 2008).

Hu and Chou (2009) synthesized albumin-imprinted polymers to separate albumin from other proteins in solution using 3-dimethylaminopropylmethacrylate and tetraethylene glycolmethacrylate. They found the adsorption capacity and selectivity of the albumin imprinted polymer as 6.02×10^{-3} g/g polymer and 99.0 %, respectively (Hu and Chou, 2009).

Andaç et al. (2012b) prepared molecularly imprinted cryogels based on poly (hydroxyethylmethacrylate). Maximum adsorption capacity of MIP composite cryogel for HSA was obtained as 683.3 mg/g cryogel from non-diluted serum. They have performed selective binding experiments in the presence of human transferrin and myoglobin competitor proteins, and concluded that synthesized composite cryogels can selectively adsorb HSA (Andaç et al., 2012).

In another study, Andaç (2013) synthesized and used molecularly imprinted supermacroporous cryogels to selectively capture HSA from human serum samples. This material has been a useful candidate for selective depletion and removal of albumin from human serum prior to a detailed proteomic analysis (Andaç, 2013).

Liu et al. (2014) prepared protein-imprinted materials using hierarchical imprinting technique called h-MIPs and applied these materials for albumin depletion directly from human serum. The maximum binding capacity of h-MIPs was calculated to be 12 mg/g, which was achieved in less than 20 minutes. The h-MIPs showed much higher selectivity for albumin, with a repression factor (IF) of about 3.6 than non-template proteins. The results show that h-MIPs prepared with hierarchical imprinting technique can be used in proteome studies as artificial antibodies to selectively deplete high-abundant proteins (Liu et al., 2014).

3. MATERIALS AND METHODS

3.1. Materials

Human Serum Albumin (HSA), Human Hemoglobin (Hb), Immunoglobulin G (IgG) and 1-vinylimidazole (VIM) were purchased from Sigma-Aldrich (St. Louis, MO, USA). 2-hydroxyethyl methacrylate (HEMA), methylene bisacrylamide (MBAA), ammonium persulfate (APS) and N,N,N',N'-tetramethylene diamine (TEMED) were supplied from BioRad. All other chemicals used in this study were supplied from Sigma-Aldrich (St. Louis, MO, USA). Required solutions were prepared using ultrapure Type 1 water (UW) with a conductivity of 18 MΩ-cm at room temperature and analytical grade reagents. All reagents were stored according to provided information and waste materials were disposed abiding by waste disposal regulations. Phosphate-buffered saline (PBS) solution is used in adsorption studies to ensure physiological conditions. Ultrasonic water bath is recommended to employ for complete dissolution of MBAA in UW. It is recommended to prepare the APS solution just a few hours before use and store it at 4 °C. Rest of the APS solution should be used within a month at most. APS solutions prepared more than one month ago may result in insufficient polymerization.

SDS-PAGE reagents and equipment are given below:

- SDS-PAGE system (Mini-PROTEAN® Tetra Handcast Systems, Bio-Rad),
- 30% Acrylamide/Bis-acrylamide: 58 g of acrylamide and 2 g of MBAA were dissolved in 200 mL of UW.
- 2 M Tris-HCl pH 8.8: 72 g of Tris-HCl was dissolved in 200 mL of UW, pH of the solution was adjusted to 8.8 and the final volume was completed to 250 mL.
- 0.5 M Tris-HCl pH 6.8: 6 g of Tris-HCl was dissolved in 80 mL of UW, pH of the solution was adjusted to 6.8 and final volume was completed to 160 mL.
- 10% APS: 25 mg of APS was dissolved in 250 µL of UW.
- 10% SDS: 5 g of SDS was dissolved in 50 mL of UW.
- TEMED.
- Isopropanol or butanol.
- Kimwipes or filter paper.
- 1X Electrophoresis Buffer: 9 g Tris Base, 43.2 g Glycine and 15 mL 10% SDS were dissolved in UW and final volume was completed to 1.5 L.

- Loading buffer (Laemmli Sample Buffer 2X): 4% SDS, 20% glycerol, 0.004% bromphenol blue, 0.125M Tris-Cl, pH 6.8, 10% 2-mercaptoethanol.
- Molecular weight standarts (10-250 kDa).
- Power supply.
- Fixing and De-Staining Solution: A mixture of 40% methanol and 10% acetic acid (v/v) was prepared.
- Coomassie Brillant Blue: 1 g Coomassie Brillant Blue Dye, 200 mL Glacial Acetic Acid, 500 mL Isopropanol, 1.3 L of UW.
- Gel imaging system.

Shimadzu Type ATX224 No. D307039788 Electronic Balance was used for weighing of chemicals and samples. Scientific Vortex Mixer (Daihan, Korea) was used to mix solutions. Model of Millipore DIRECT-Q®3 ultrapure (type 1) water with BioPak®ultrafiltration cartridge with Millipak®Express 20 (0.22 μm) membrane filter was used for water system. Nanodrop 2000c Spectrophotometer were purchased from Thermo Scientific (USA) and used for quantification and assessment of proteins of interest, to examine adsorption capacity, selectivity and other characterisics of obtained cryogel columns. Morphology of synthesized columns were characterized by SEM (JEOL JSM 5600, Jeol Co.,Tokyo, Japan) and Micro-CT analysis. Adsorption, desorption and washing processes were performed in a continuous system using peristaltic pump.

It has not been required to list basic laboratory equipment. Given amounts of reagents are for synthesizing approximately 0.24 g (dry weight) of each HSA-DIP. Double-layer imprinted polymers can be synthesized for a wide variety of purposes, employing different types of molecules as the template. Nevertheless, the experimental conditions (i.e. temperature, flow rate, buffers and solutions) may vary from one molecule to another and should be optimized according to the molecule of interest. This protocol has been carried out under different experimental conditions and the optimized protocol has been performed within the scope of this thesis study.

3.2. Methods

In this study, HSA double-imprinted polymers (HSA-DIP) were synthesized for the selective HSA adsorption from aqueous media and further HSA depletion studies in human serum. HSA-

DIP cryogel columns were prepared using different ratios of cross-linker, functional monomer and target molecule, and were characterized by swelling tests, SEM and Micro-CT analysis.

After the synthesis of double-layer imprinted polymers, the template molecule (HSA) was eluted using salt-containing buffers from the regions where they are attached, thereby creating HSA-specific regions in the structure of the polymer. Following the template removal step, adsorption of HSA from aqueous solutions was examined using template-free HSA-DIPs. In addition, the adsorption properties of HSA-DIPs against competing molecules were examined and the selectivity of the material was discussed. Finally, double-layer non-imprinted columns (DL-NIP) without HSA and HSA-imprinted cryogels with different monomer concentrations (HSA-MIP$_{\%8}$ and HSA-MIP$_{\%16}$) were synthesized for control and the results obtained were compared. Selectivity studies were performed against Hb and IgG proteins in physiological condition (PBS pH 7.4) and HSA depletion directly from human serum was studied in order to demonstrate the specificity of the HSA-DIP for HSA. In addition, HSA-DIPs were examined in terms of reusability.

3.2.1. Synthesis of HSA-Specific Double-Imprinted Polymers (HSA-DIPs)

The synthesis steps of HSA double-imprinted columns (HSA-DIP) that can specifically recognize HSA, double-layer non-imprinted columns (DL-NIP) without HSA and HSA-imprinted cryogels prepared separately with different monomer concentrations (HSA-MIP$_{\%8}$ and HSA-MIP$_{\%16}$) are described below.

For the first layer of the cryogel with 8% monomer concentration (w/w): HSA-VIM pre-complex was prepared by dissolving HSA molecules and VIM functional monomers (1/10 molar ratio) in 1 mL of UW and left at 4 °C for at least 4 hours, to allow secondary interactions between HSA and VIM to occur. 0.65 mL of HEMA was dissolved in 5 mL of UW and 137.5 mg of MBAA were dissolved in 10 mL of UW. These two solutions were mixed together and stirred in ice-bath using a magnetic stirrer. 1 mL of pre-complex was added into the HEMA-MBAA mixture. APS and TEMED [1% (w/v) of the total monomers] were added into the final mixture and the total polymer solution were mixed for 5 minutes in the ice bath. This mixture was equally divided into 10 mL syringes (id. 14.5 mm) with closed outlets at the bottom (3 mL polymer solution to each syringe), and the syringes were fixed in an upright position and frozen in the cryostat at -16 °C. Macroporous columns were kept in the deep-freezer at -20 °C for 24

hours to complete the polymerization process. After the polymerization process, the polymers taken from the freezer were allowed to reach room temperature. The water content frozen in the columns, were thawed at room temperature and interconnected macroporous structure were obtained.

The same procedure was applied for the synthesis of the second layer with 16% monomer concentration (w/w), except that the amount of ingredients excluding water were doubled. HSA-VIM pre-complex was prepared by dissolving HSA molecules and VIM functional monomers (1/10 molar ratio) in 1 mL of UW and left at 4 °C for at least 4 hours, to allow interactions between HSA and VIM to occur. 1.3 mL of HEMA was dissolved in 3.5 mL of UW and 275 mg of MBAA were dissolved in 10 mL of UW. These two solutions were mixed together and stirred in ice-bath using a magnetic stirrer. 1 mL of pre-complex was added into the HEMA-MBAA mixture. APS and TEMED [1% (w/v) of the total monomers] were added into the final mixture and the total polymer solution were mixed for 5 minutes in the ice bath. Then, the polymer solution was divided equally to 10 mL syringes (id. 14.5 mm) with closed outlets at the bottom (3 mL polymer solution to each syringe). Squeezed cryogels with 8% monomer concentration were immersed into the polymer solution in the syringes to swell. The syringes were fixed in an upright position and the polymeric system was frozen in the cryostat at -16 °C. HSA-DIP columns were kept in the freezer at -20 °C for 24 hours to complete the polymerization process. After the polymerization process was completed, HSA-DIP columns were removed from the freezer and allowed to reach room temperature. Frozen water content in the columns was thawed at room temperature, and HSA-DIP columns with interconnected pores were obtained (see Figure 3.1).

DL-NIP columns were synthesized by the same procedure, in presence of VIM only, instead of HSA-VIM pre-complex. HSA-$MIP_{8\%}$ and HSA-$MIP_{16\%}$ columns were synthesized separately with the monomer concentration of 8% and 16%, respectively, in the presence of HSA. DL-NIP, HSA-$MIP_{8\%}$ and HSA-$MIP_{16\%}$ columns were used as control groups in the adsorption studies. All the columns were washed with methanol/water mixture (70/30, v/v) for 48 hours at room temperature in order to remove unreacted monomers and other undesired components.

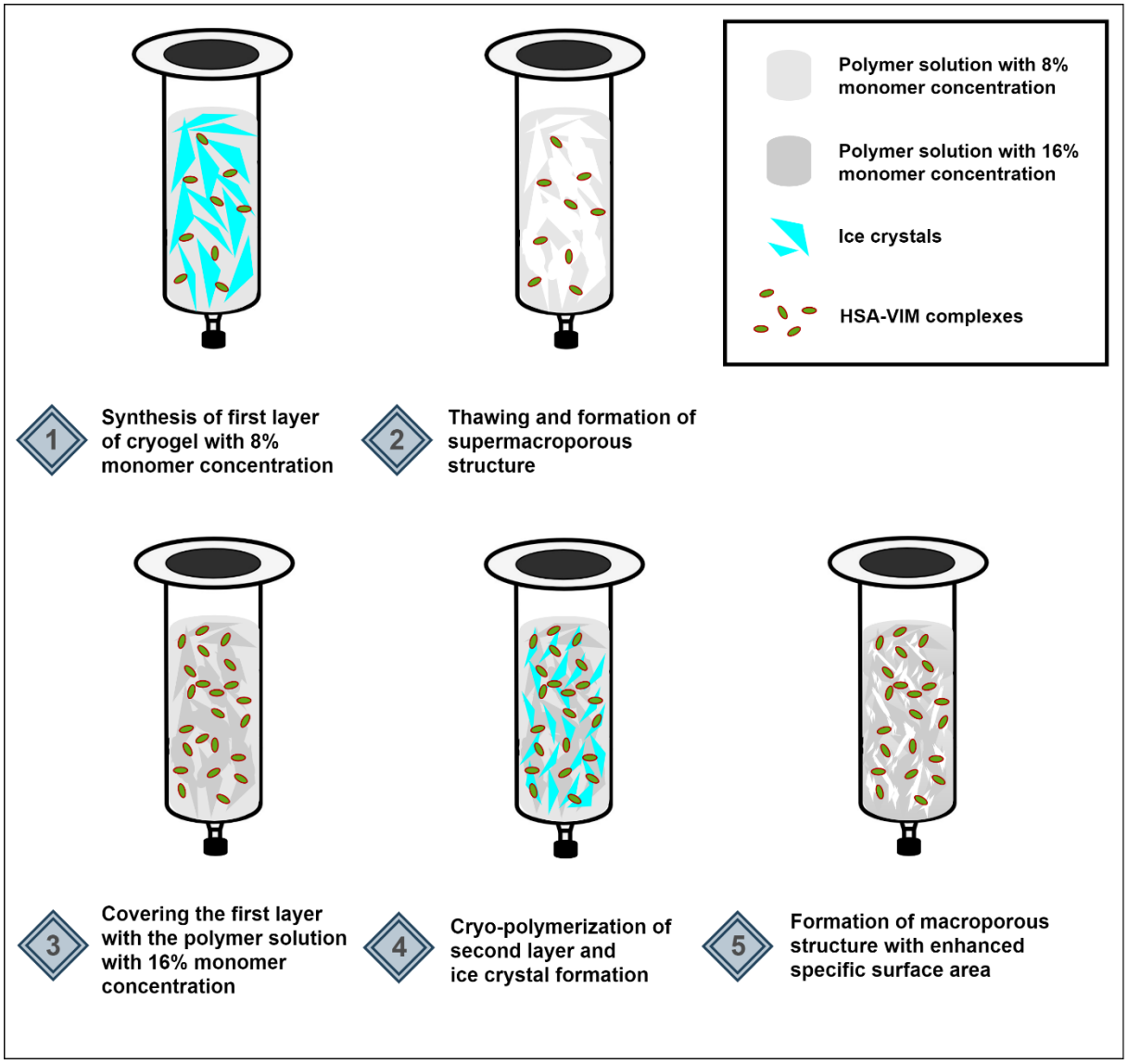

Figure 3.1. Double-Layer Imprinting Technique. Synthesis steps of HSA double-imprinted cryogel columns (HSA-DIP).

3.2.2. Template Removal Studies

10 mL of elution agent (0.5 M NaCl in PBS pH 7.4) was passed through HSA-DIP columns in a continuous system using a peristaltic pump. After each elution cycle, HSA leakage was analyzed by measuring absorbance at 204 nm using UV spectrophotometer. Elution step was repeated until no HSA molecule was observed in the final solution. HSA-DIP columns, in which HSA was removed, were washed with ethanol and water for 12 hours at room temperature (see Figure 3.2).

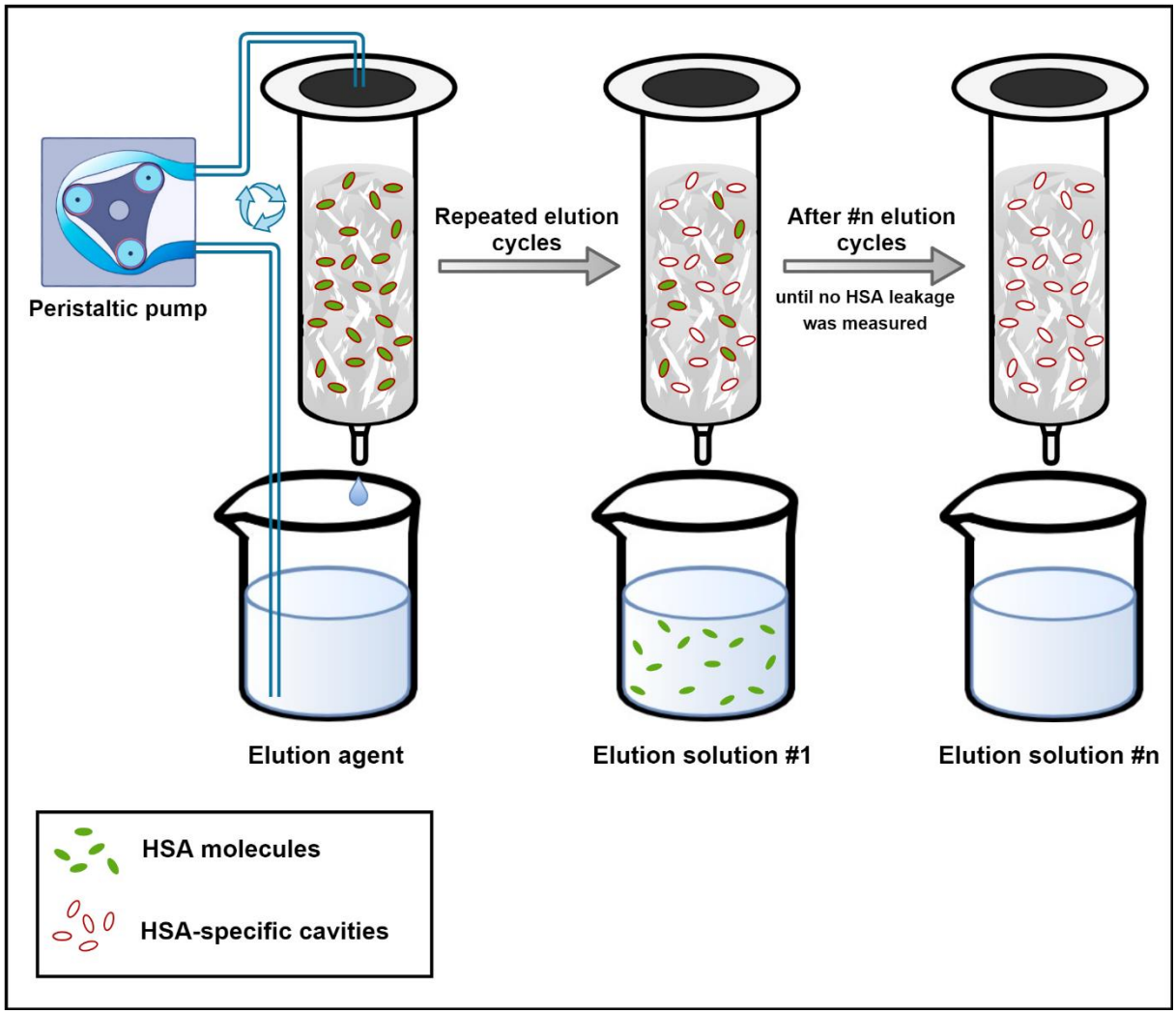

Figure 3.2. Template Removal. Schematic representation of template removal followed by formation of template-specific cavities.

3.2.3. Characterization Studies

Swelling ratio of HSA-DIP and DL-NIP columns were determined by swelling tests. The polymerization yield of the macroporous columns were calculated using polymerization feed amounts and dry gel weight. The surface and bulk structures of the columns were examined by SEM, since SEM provides high magnification. In addition, Micro-CT analysis was performed for further assessment of morphology of synthesized cryogel columns.

3.2.3.1. Swelling Tests

Swelling behaviours of the synthesized columns (HSA-DIP, DL-NIP, HSA-MIP$_{8\%}$, HSA-MIP$_{16\%}$) were evaluated in UW. Firstly, cryogel samples were swollen in UW and frozen at -20 °C, then, lyophilized for 24 h at 0.001 mbar and -50 °C. Dry weight of cryogel samples was

determined. Samples were taken into a falcon containing UW and ambient temperature was fixed to 25 °C using an isothermal water bath. After 2 h, samples were carefully taken and excess water around samples were removed using a piece of filter paper. Swollen weight of samples was determined and recorded at three-hour intervals. After 24 h, final weight of samples was recorded. The water content of the cryogel was calculated by using the following equation.

$$\text{Water uptake ratio \%} = [(W_s - W_0) / W_0] \times 100 \quad (1)$$

W_0 and Ws are the weights of cryogel samples before and after swelling, respectively.

Swollen samples (1 mL) were placed in an oven at 60 °C. Weight of samples were determined and recorded at regular intervals until there was no difference between consecutive weighing. Dry samples were weighed, and dry mass was recorded (m_{dried}). The polymerization yield was calculated using the following equation.

$$\text{Polymerization Yield (\%)} = (m_{dried} / m_t) \times 100 \quad (2)$$

In this equation, m_t stands for the total mass of the monomers in the feed polymer mixture.

In order to evaluate macroporosity of swollen columns, samples were squeezed carefully and the water content inside the macropores were removed. Squeezed samples were weighed ($m_{squeezed}$) and the total volume of macropores was approximately determined using the following equation.

$$\text{Macroporosity (\%)} = (m_{swollen} - m_{squeezed})/m_{swollen} \times 100\% \quad (3)$$

During the swelling test, all measurements were made at least three times. Average values were calculated and interpreted.

3.2.3.2. Surface Morphology

Scanning electron microscopy was employed, to analyze the structure of synthesized columns. When collecting samples for SEM from dried columns, it is important to take a piece from

inside, instead of taking samples from external parts. Samples from the outer surface which is artificially smooth, may be misleading. Internal macro- and microporous structure is reflected best, only when the outer part of the material is cut, and the inner sample is taken. 2.5 % glutaraldehyde was used for the fixation of samples overnight, followed by freeze-drying step at -50 °C (Lyophilizer, Christ Alpha 1-2 LD plus, Germany). Finally, sputter coating of samples with gold-palladium alloy (40/60) was performed and examined using a JEOL JSM 5600 scanning electron microscope (Tokyo, Japan). Surface area measurements were performed via mercury porosimetry.

Micro-CT analysis was performed for further assessment of morphology. Micro-CT analysis uses X-rays to obtain two-dimensional images from the sample. These two-dimensional images were loaded into the CT Analyzer (SkySkan 1272, Version: 1.18.4.0) software to create a 3-dimensional structure, and the pore size and distribution of these pores were calculated.

3.2.4. Adsorption Studies

HSA adsorption properties of HSA-DIP, DL-NIP, HSA-MIP$_{\%8}$ and HSA-MIP$_{\%16}$ columns were performed from the aqueous HSA solution (in PBS pH 7.4) in a continuous system at 25 °C. The effect of equilibrium HSA concentration (0.5-10 mg/mL), interaction time (0-120 min) and flow rate (0.1-2 mL/min) on HSA adsorption were examined.

Template-free HSA-DIP column and DL-NIP column were equilibrated with 10 mL of PBS pH 7.4 for 30 min using a peristaltic pump. For the evaluation of the effect of equilibrium HSA concentration on adsorption capacity, varied concentrations of HSA solutions within the range of 0.5-10 mg/mL (V: 10 mL) were passed through the column one by one in a continuous system at a flow rate of 0.5 mL/min at 25 °C for 2 h. Amount of adsorbed HSA were measured spectrophotometrically by monitoring the decrease in absorbance value at 204 nm. After desorption and re-equilibriation of columns, effect of flow rate on HSA adsorption property of HSA-DIP column was examined within the range of 0.1-2 mL/min. 5 mg/mL HSA solutions (pH 7.4, 10 mL) were passed through the column one by one at different flow rates in a continuous system at 25 °C for 2 h. Amount of adsorbed HSA were measured spectrophotometrically by monitoring the decrease in absorbance value at 204 nm, following by re-equilibriation of columns. Evaluation of the effect of interaction time on HSA adsorption was performed by passing with 10 mL of PBS pH 7.4 through HSA-DIP column in a continuous

system at a flow rate of 0.5 mL/min at 25 °C for 2 h, taking 50 µL of samples at certain intervals (0, 5, 10, 15, 30, 45, 60, 90, 120 min). Amount of adsorbed HSA for each time were measured spectrophotometrically by monitoring the decrease in absorbance value at 204 nm. Additionally, the effect of monomer concentration as well as the double-layer imprinting technique on maximum HSA adsorption of columns was investigated under optimized conditions, using HSA-imprinted polymers with different monomer concentration HSA-DIP, HSA-MIP$_{\%8}$ and HSA-MIP$_{\%16}$. For this purpose, 10 mL of 5 mg/mL HSA solution in PBS pH 7.4 was passed through the columns for 2 h at a flow rate of 0.5 mL/min.

$$Q= [(C_0-C)\ V]/m \quad (4)$$

Here, Q is the amount of adsorbed HSA onto unis mass of columns (mg/g); C_0 is the initial HSA concentration; C is HSA concentration after treatment for 2 h, respectively (mg/mL); V is the volume of the aqueous phase (mL); and m is the dry mass of the column (g). Each experiment was performed three times for quality control and statistical calculations.

Experimental adsorption data were further used for investigating the interaction behavior between the DIP and the HSA molecules via adsorption isotherms. The adsorption isotherms basically reveal the relationship between the amount of adsorbate adsorbed on the adsorbent (qe) and the equilibrium concentration of the adsorbate in the solution (Ce). In this study the interactions were investigated using Langmuir and Freundlich adsorption isotherm models and suitability of adsorption property of HSA-DIP to these isotherms is evaluated.

Adsorption mechanism was explained using adsorption kinetics models. The experimental time-adsorption amount data were applied to first and second order kinetic models to determine the mechanisms, which control the adsorption process ie. mass transfer or chemical reaction. Calculations were made for pseudo first order kinetics and pseudo second order kinetics and suitability of binding kinetics between HSA and HSA-DIP to these models is evaluated.

3.2.5. Selectivity Studies

Selective HSA adsorption property of synthesized columns were analyzed, performing a selectivity experiment as compared to competitor molecules: Hb and IgG. Three separate solutions of HSA, Hb and IgG with the concentration of 5 mg/mL in 10 mL of PBS pH 7.4,

were prepared in order to evalute selectivity spectrophotometrically and also a solution of HSA and competitors together in the same environment (HSA-Hb-IgG solution: 4 mg of each molecule in 10 mL of PBS pH 7.4) was prepared for further assessment of the selective adsorption property of HSA-DIP columns (see Figure 3.3)

10 mL of each solution was passed through HSA-DIP columns in a continuous system at a flow rate of 0.5 mL/min at 25 °C for 2 hours using a peristaltic pump. 1 mL of sample was taken before and after adsorption for each solution. The concentration of absorbed molecules were determined spectrophotometrically at 204 nm and distribution coefficient (Q_d, mL/g) was calculated according to the following equation.

$$Q_d = [(C_i - C_f) / C_f] \text{ x } V / m_{dry} \quad (5)$$

Imprinting factor (IF) for HSA and competitors were calculated using the following equation, in order to evaluate selective adsorption property of HSA-DIP columns.

$$IF = Q_{d\ HSA\text{-}DIP} / Q_{d\ DL\text{-}NIP} \quad (6)$$

In this equation, $Q_{d\ HSA\text{-}DIP}$ and $Q_{d\ DL\text{-}NIP}$ refer to the distribution coefficients of HSA-DIP and DL-NIP columns, respectively.

Selectivity of HSA-DIP columns for the template molecule is evaluated by interpreting the selectivity coefficient (k) of competitors. “k” values of each competitor were calculated according to the following equation.

$$k = Q_{d\ HSA\text{-}DIP}(\text{template}) / Q_{d\ HSA\text{-}DIP}(\text{competitor}) \quad (7)$$

$Q_{HSA\text{-}DIP}$(template) and $Q_{HSA\text{-}DIP}$(competitor) refers to the distribution coefficients of the template and each competitor molecule in the HSA-DIPs.

HSA depletion studies from human serum: HSA-DIP columns were equilibrated by applying 20 mL of PBS solution for 30 min before serum application. Then, 10 mL of the commercially obtained human serum circulated through the HSA-DIP column for 1 h at room temperature at

constant flow rate of 0.5 mL/min by peristaltic pump. 2 mL of serum samples were taken before and after the interaction of serum with HSA-DIP column. Then, 10 mL of PBS as washing solution was applied to HSA-DIP column to remove non-specifically attached HSA. The depleted HSA amount was determined via determining HSA adsorption amount onto HSA-DIP column by measuring the initial, and final concentration of HSA in serum and washing solution (Adana City Hospital, Adana). In this study, non-diluted human serum, and 1/2 and 1/10-fold diluted (using PBS pH 7.4) human serum were examined.

3.2.5.1. SDS-PAGE

Further assessment of the selective HSA adsorption property of HSA-DIPs were achieved by performing a suitable SDS-PAGE protocol, with a monomer concentration of 12% (w/v) and employing a protein ladder within the range of 10-200 kDa, since molecules of interest have molecular weights within this range (HSA: 67 kDa, Hb: 16 kDa x four subunits, IgG: two identical light chains about 25 kDa and two identical heavy chains about 50 kDa).

For the synthesis of running gel with a monomer concentration of 12%: 7.2 mL of 30% acrylamide/bis-acrylamide, 3.38 mL of 2 M Tris-HCl (pH 8.8), 180 µL of 10% SDS and 7 mL of UW were mixed together, and gently homogenized by pipetting in order to prevent possible foaming caused by SDS. Finally, 180 µL of 10% APS and 20 µL of TEMED was added into the solution and final solution was gently mixed twice by inversion. Since APS plays a role as initiator and TEMED acts as catalyst, these substances should be added into the polymeric solution last, just before pouring the gel. Final solution was poured between two glass-plates until the line which is 1 cm away from the end of the comb or 2 cm away from the top point of the glass plates, was reached. To obtain a smooth gel and to get rid of air bubbles, butanol was added immediately after the gel was poured. Also, polymerization is inhibited by oxygen, and the butanol isolates the gel from the air. The gel was then left for polymerization at room temperature for at least 15 minutes. After this process, butanol was removed by turning gel apparatus upside down carefully, and then using Kimwipes to completely remove the remaining butanol in the space between two glass-plates.

For the synthesis of stacking gel with a monomer concentration of 4%: 0.7 mL of 30% acrylamide/bis-acrylamide, 1.5 mL of 0.5 M Tris-HCl (pH 6.8), 60 µL of 10% SDS and 4 mL of UW were mixed together. Finally, 50 µL of 10% APS and 10 µL of TEMED was added into

the solution and final solution was gently mixed twice by inversion. Polymeric solution was poured between two glass-plates until the top point of the glass plates. An SDS-PAGE comb was inserted into the stacking gel between glass plates in order to create wells. Then, polymeric system was allowed to polymerize at room temperature for at least 20 minutes.

Preparation of samples, loading into the wells and running process: Gel with glass-plates was taken into the gel running box. 1X electrophoresis buffer was poured into the box, first over the wells to cover the gel, then outside of the plates until specified point and the comb was carefully removed. 7.5 μL of loading buffer and 7.5 μL of protein sample were mixed together. Each sample was boiled for 10 minutes to obtain denatured proteins. Following protein samples and protein ladders were prepared and 15 μL of these samples were run in SDS-PAGE:

1. Protein ladder within the range of 10-200 kDa.
2. HSA-Hb-IgG solution (Adsorption initial).
3. Adsorption final solution of HSA-Hb-IgG solution.
4. Desorption solution of HSA-Hb-IgG solution.
5. Diluted serum (Adsorption initial).
6. Adsorption final solution of diluted serum.
7. Desorption solution of diluted serum.
8. Protein ladder within the range of 10-200 kDa.

Samples were run at 60 volts for about 1-2 hours using a power supply, until visible dyes which were loaded into the gel together with samples, were observed to reach at the bottom of the gel. Running a gel at a higher voltage than what is required, results in “smiling bands” on the gel, due to the relatively fast movement of middle part of a sample than both ends of the band. It is important to determine a proper voltage for the running process of a given gel.

Fixing, staining and de-staining steps: Obtaining gel was seperated from glass-plates and stacking gel was removed gently. Remaining gel (running gel) was washed with a mixture of methanol and acetic acid in a shaker for at least 30 minutes and washed with distilled water for a while in order to fix the location of protein samples inside the gel. Then, the gel was taken into diluted Coomassie Brillant Blue dye and shaked for at least 4 hours, allowing the dye to go through the porous structure of polyacrylamide gel, and to reach and bind to the fixed protein samples. Then, fixing solution was used for the de-staining process. De-stanining process was

carried out in order to allow excess dye inside and outside of the gel to be removed, except dye that binds to proteins, so that, proteins appeared as clear bands.

Gel imaging system: The gel was visually analyzed using a gel imaging system.

3.2.6. Desorption and Reusability

10 mL of desorption agent (0.5 M NaCl in PBS pH 7.4) was passed through HSA-DIP columns in a continuous system at a flow rate of 0.5 mL/min at 25 °C for 2 hours using a peristaltic pump, to desorb adsorbed molecules. HSA leakage was analyzed by measuring absorbance using UV spectrophotometer at 204 nm, blanking with desorption agent. The desorption rate was calculated using the following equation.

$$\text{Desorption rate (\%)} = \frac{\text{The amount of HSA released into the desorption medium}}{\text{The amount of adsorbed HSA molecules}} \times 100 \quad (8)$$

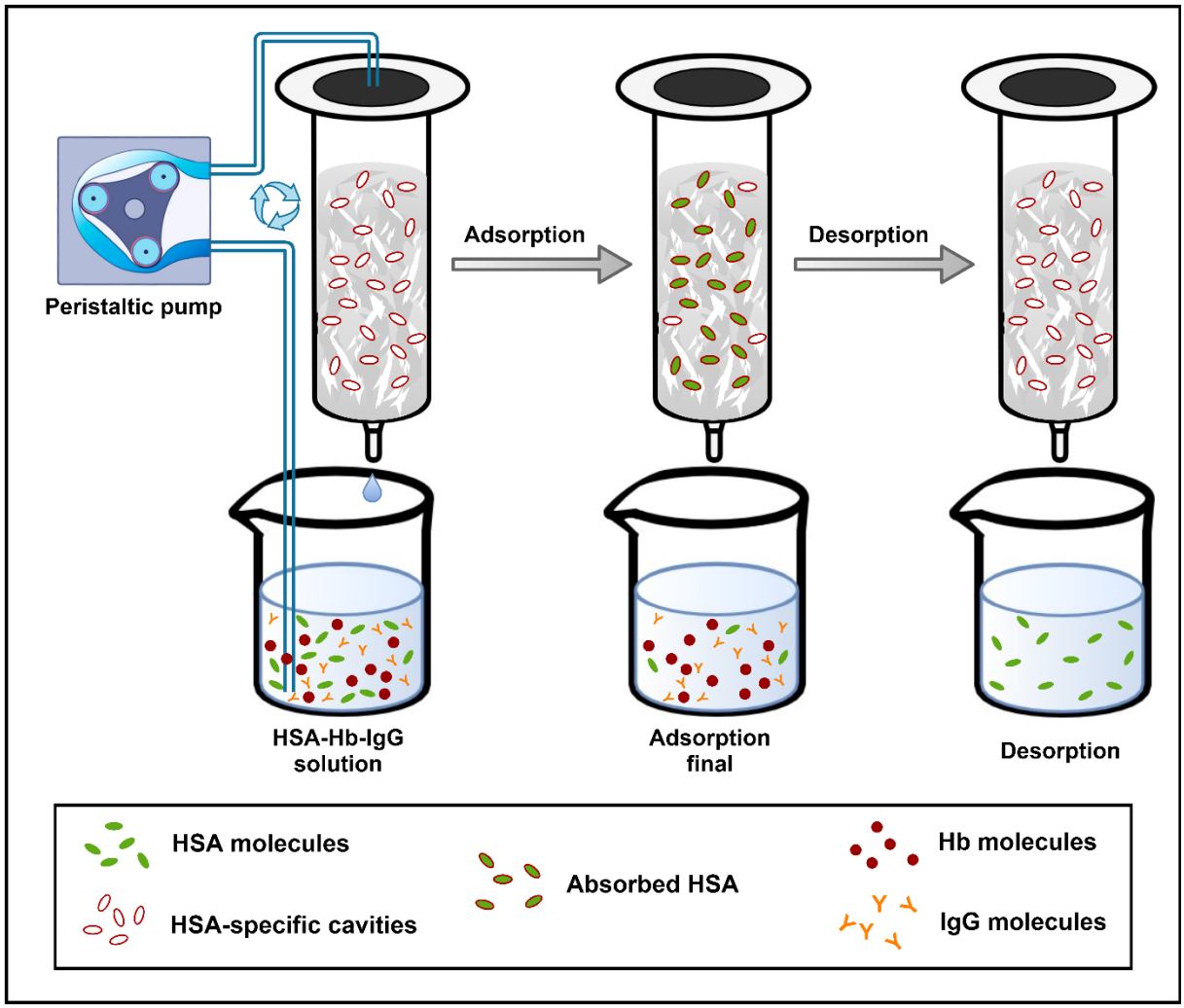

Figure 3.3. Selectivity Studies. Representative illustration of experimental set up of selevtivity studies.

4. RESULTS AND DISCUSSIONS

Depletion of high-abundant proteins such as HSA, Hb, etc. in human blood, is generally the first step in serum- and plasma-based proteomics studies, where the diagnosis of potential protein biomarkers often present in low amounts is the main goal. Within the scope of this thesis study, HSA-DIP columns were synthesized to be tested for the selective HSA adsorption from aqueous solutions and depletion of HSA directly from human serum, for further use in proteomics applications.

HSA imprinted cryogel was synthesized with the monomer concentration of 8%, and after cryogelation process at -16°C in freezer for 24 hours, the polymeric system was left to thaw at room temperature. Then, repeated washing steps were performed using UW. The second HSA imprinted polymeric solution with the monomer concentration of 16% were prepared and immediately poured down to the first cryogel. We expected to see that the second polymeric solution were polymerized inside the macroporous structure of the first one, so that the surface area will increase. Double-layer non-imprinted columns (DL-NIP) without HSA and HSA-imprinted cryogels with different monomer concentrations (HSA-MIP$_{\%8}$ and HSA-MIP$_{\%16}$) were synthesized for control (see Figure 4.1).

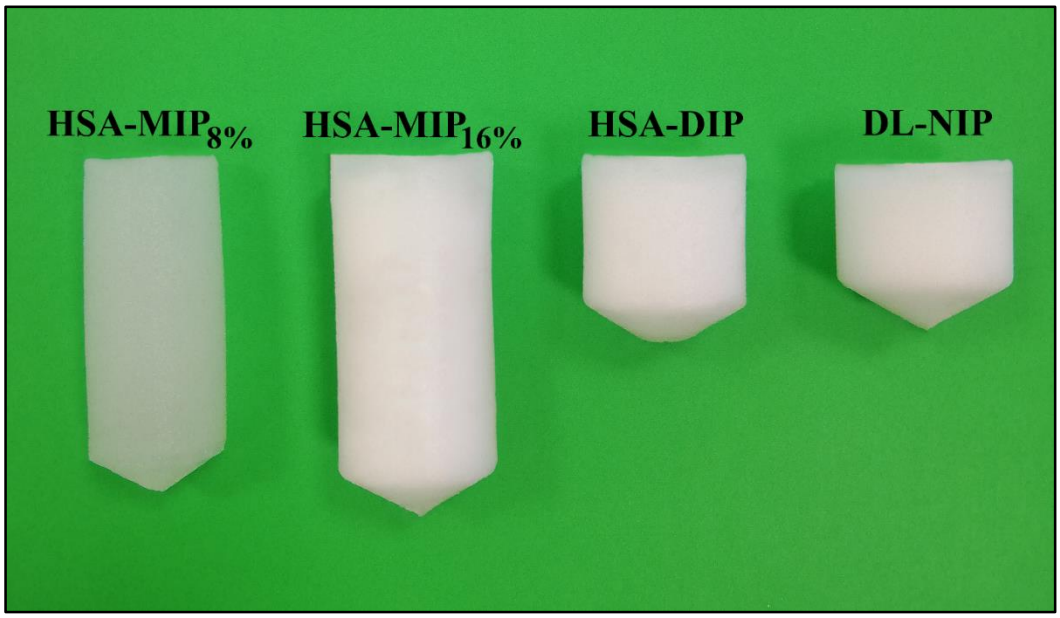

Figure 4.1. Cryogel Columns. Optical photographs of cryogel columns with different monomer concentrations: HSA-MIP$_{8\%}$, HSA-MIP$_{16\%}$, HSA-DIP and DL-NIP.

4.1. Template Removal

Elution agent (0.5 M NaCl in PBS pH 7.4) was used to remove the template molecule from the HSA-DIP column in order to obtain template-specific cavities. After four cycles of elution, about 90% of HSA molecules were removed from the cavities and cavities in the structure of HSA-DIP were formed that can selectively bind to HSA.

4.2. Characterization Studies

Swelling rate, porosity and polymerization yield were determined by swelling tests (see Table 4.1 and Figure 4.2).

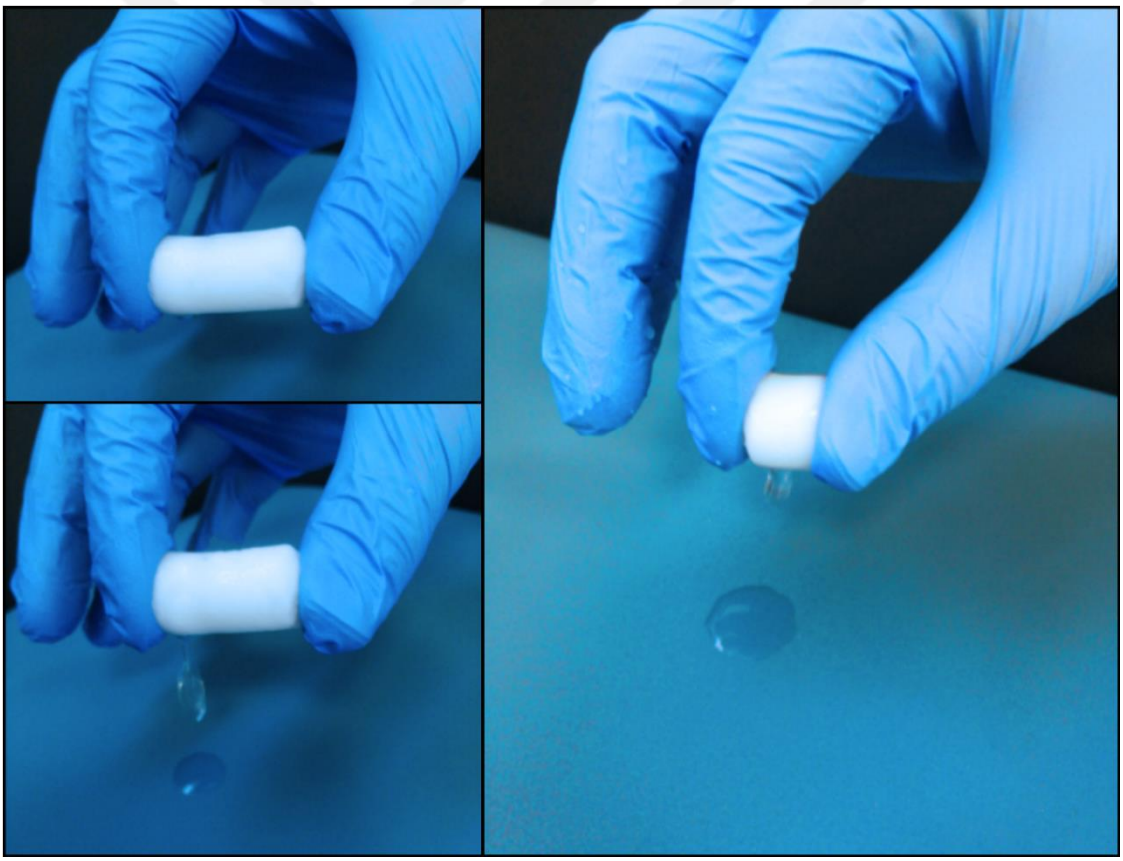

Figure 4.2. Cryogel Columns. Elastic morphology of cryogel columns.

Table 4.1. Swelling tests. Swelling rate, polymerization yield, porosity and surface area of HSA-MIP$_{8\%}$, HSA-MIP$_{16\%}$, HSA-DIP and DL-NIP.

Polymers	**Swelling Rate, %**	**Polymerization Yield, %**	**Porosity, %**	**Surface Area, m^2/g**
HSA-MIP$_{8\%}$	89	92	92	12
HSA-MIP$_{16\%}$	88	90	90	21
HSA-DIP	84	95	86	39
DL-NIP	82	95	84	37

Cryogels draw attention by their relatively reduced flow resistance, shorter diffusion distance, etc. features and macroporous morphology which makes it easier to study with viscous and heavy fluids with particles without blocking the cryogel column (Noppe et al., 2007; Lozinsky et al., 2003; Dainiak et al., 2007; Kumar and Srivastava, 2010; Baydemir and Denizli, 2015). However, the adsorption capacity of the cryogels for proteins is low due to the interconnected supermacropores within the matrix (i.e., low surface area). Improving the binding capacity of supermacroporous cryogels has a great importance in a bioseparation process (Dainiak et al., 2007; Kumar and Srivastava, 2010). According to results of swelling tests, it was concluded that the polymeric solution with 16% monomer concentration polymerized in the macroporous structure of the first layer of cryogel with 8% monomer concentration for double-layer columns (HSA-DIP and DL-NIP), thus achieving relatively higher surface areas as compared to monolayer columns. This is an excellent result for enhancing specific interaction areas between HSA and HSA-DIP. The surface and bulk structures of the prepared columns were examined by scanning electron microscopy (SEM) due to their high magnification (see Figure 4.2). Approximate measurements of pore sizes of four different HEMA-based cryogel columns were performed with Image J program using SEM images (see Figure 4.3) with at least 20 different pores from samples at 100x magnification (summarized in Table 4.2 and Figure 4.4).

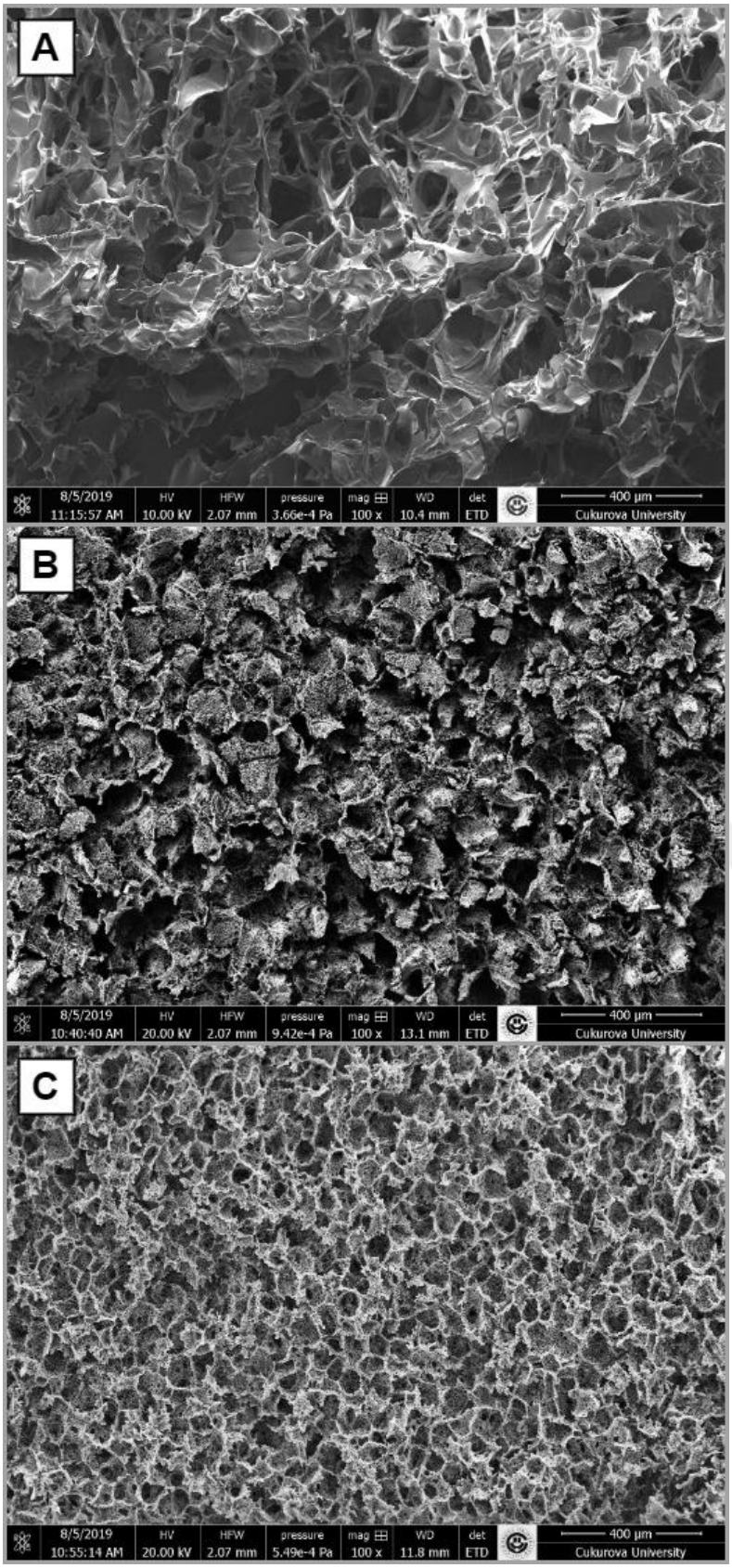

Figure 4.3. SEM Analysis. SEM photographs of A) HSA-MIP$_{8\%}$, B) HSA-MIP$_{16\%}$, and C) HSA-DIP cyrogel columns.

Table 4.2. Pore Size Distribution. Approximate pore sizes of HSA-MIP$_{8\%}$, HSA-MIP$_{16\%}$ and HSA-DIP.

Polymers	Approximate pore size id., µm
HSA-MIP$_{8\%}$	136.19 µm ± 28.93 µm
HSA-MIP$_{16\%}$	89.75 µm ± 7.39 µm
HSA-DIP	65.76 µm ± 16.81 µm

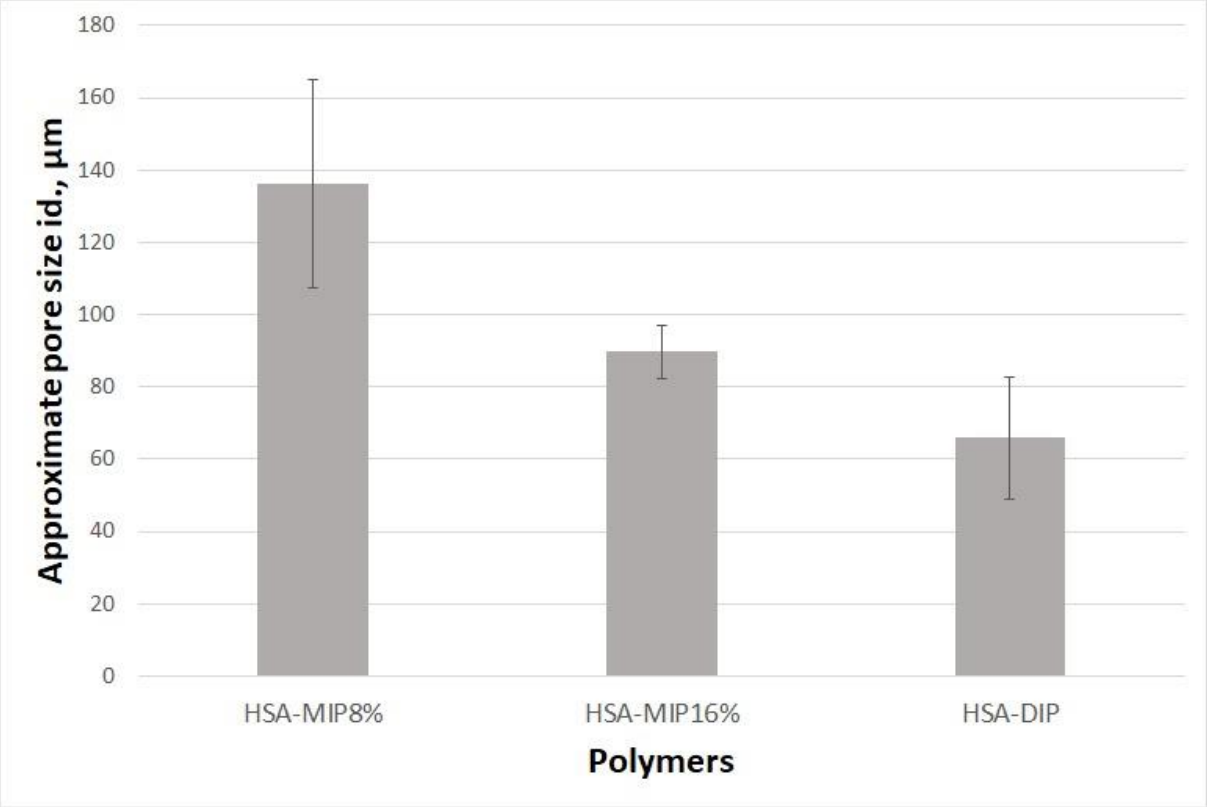

Figure 4.4. Pore Size Distribution. Approximate pore sizes of HSA-MIP$_{8\%}$, HSA-MIP$_{16\%}$ and HSA-DIP.

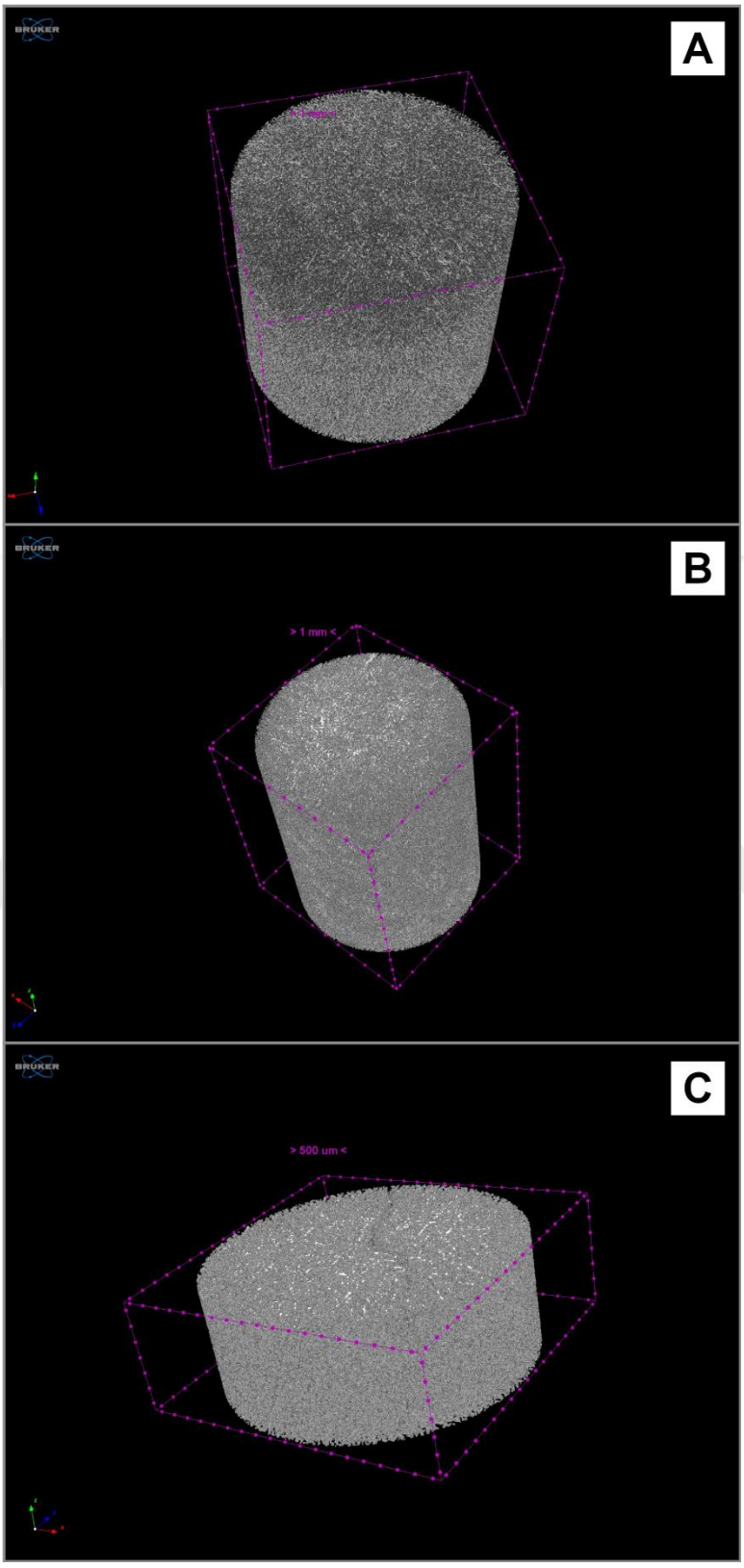

Figure 4.5. Micro-CT analysis. Micro-CT photographs of A) HSA-MIP$_{8\%}$, B) HSA-MIP$_{16\%}$, C) HSA-DIP columns.

In addition to the evaluation of interconnected pores by SEM analysis and the determination of macroporosity by swelling tests; the distribution of the pores, macropore volume and the size of the pores and the interconnection are clear as a result of Micro-CT analysis.

Figure 4.5 shows the Micro-CT photographs of HSA-MIP$_{8\%}$, HSA-MIP$_{16\%}$ and HSA-DIP column. Micro-CT analysis uses X-rays to obtain two-dimensional images from the sample. These two-dimensional images were loaded into the CT Analyzer (SkySkan 1272, Version: 1.18.4.0) software in order to create a 3-dimensional structure, and the pore size and distribution of these pores were calculated.

It was observed that 99% of HSA-MIP$_{\%8}$ had a trabecular thickness distribution between 15 and 47 μm and similarly 100% of HSA-MIP$_{\%16}$ had a trabecular thickness distribution between 15 and 47 μm. Whereas, these values were reported higher for HSA-DIP; 99.9 % of HSA-DIP had a trabecular thickness distribution between 21 and 63 μm. Total porosity was calculated as 96.5, 96.5 and 89 % for HSA$_{\%8}$, HSA$_{\%16}$ and HSA-DIP. It is clear that the trabecular thickness increased by covering HSA$_{\%8\ MIP}$ layer with second HSA$_{\%16}$ layer.

4.3. Adsorption Studies

4.3.1. Effect of Equilibrium HSA Concentration on HSA Adsorption

The initial HSA concentration was varied in the range of 0.1-10 mg/mL and the HSA adsorption capacity of the columns was examined. The maximum HSA adsorption for HSA-DIP and DL-NIP polymers was calculated as 106.8 mg and 5.14 mg per gram polymer, respectively (see Figure 4.6).

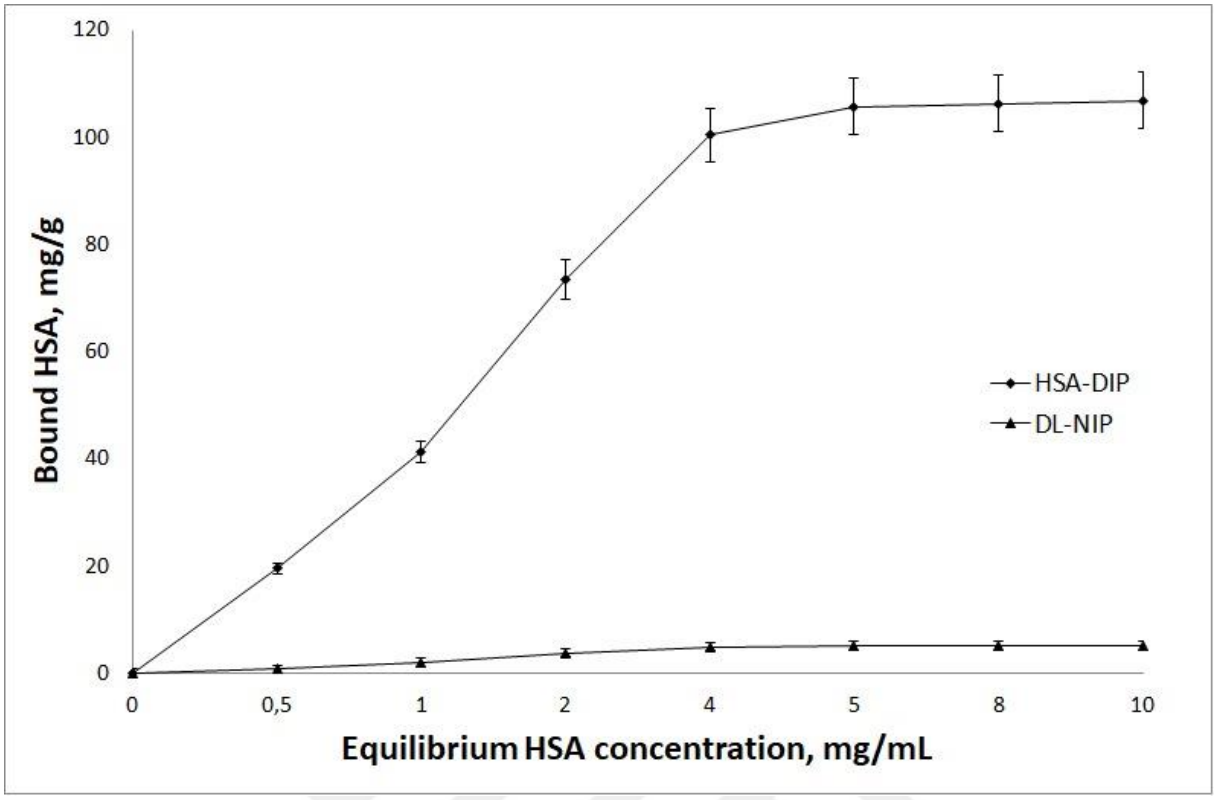

Figure 4.6. Effect of equilibrium HSA concentration on HSA adsorption. Maximum HSA adsorption of HSA-DIP and DL-NIP was calculated as 106.8 mg/g and 5.14 mg/g, respectively. m_{dry}: 0.24 g, V: 10 mL, time: 120 min, pH: 7.4, flow rate: 0.5 mL/min.

Experimental adsorption data were used for investigating the interaction behavior between the DIP and the HSA molecules via adsorption isotherms. The adsorption isotherms basically reveal the relationship between the amount of adsorbate adsorbed on the adsorbent (Qe) and the equilibrium concentration of the adsorbate in the solution (C_e) (Yıldırım and Peşint, 2020). In this study the interaction was investigated using Langmuir and Freundlich adsorption isotherm models.

Langmuir isotherm describes the adsorption process as a single layer and it is assumed that the adsorbent surface is homogeneous. Irwing Langmuir in 1918 suggested that all binding sites on the adsorbent surface are thermodynamically co-energetic and only one adsorbate molecule can bind to each binding site. As a result, the surface thickness increases only one binding atom size of an adsorbate molecule as a result of adsorption. Langmuir adsorption isotherm expressed as follows (Labrou and Clonis, 1995; Yıldırım and Peşint, 2020).

$$Q = Q_{max} * b * C_e / (1 + b * C_e) \quad (9)$$

In here Q is the HSA binding capacity of the adsorbent mg/mL, C_e equilibrium concentration of HSA (mg/L), b is Langmuir constant (mL/mg), Q_{max} is the highest HSA adsorption capacity (mg/g). Equation 9 Linearized as equation 10 and C_e/Q plotted versus against C_e to obtain $1/Q_{max}$ and $1/Q_{max}$*b from cut-off point and slope (see Figure 4.7A) (Ali and Mahmud, 2015; Martínez-Vertel, 2019; Yıldırım and Peşint, 2020).

$$C_e / Q = 1 / (Q_{max}.b) + (C_e / Q_{max}) \quad (10)$$

Freundlich adsorption model describes adsorption process as multilayer and it is assumed that the that the adsorbent surface is heterogeneous. German Physicochemist Herbert Max suggests all binding sites on the adsorbent surface are not equally energized and each binding site can bind more than one adsorbate molecules (Finette et al., 1997; Yıldırım and Peşint, 2020).

Freundlich adsorption isotherm expressed exponential as in equation 11.

$$Q_e = Q_f * C_e^{1/n} \quad (11)$$

In this equation, Q_e is the HSA adsorption amount (mg/g) and C_e is the equilibrium HSA concentration in the solution (mg/L). Q_f is maximum Freundlich HSA adsorption capacity in mg/g and 1/n is Freundlich constants indiates adsorption intensity. This equation can be linearized by taken logarithm both sides of the eqution. The $\ln C_e$ was plotted against $\ln Q_e$ to obtain 1/n and Q_f values, cut-off point and slope (see Figure 4.7B) (Finette et al., 1997; Ali and Mahmud, 2015; Martínez-Vertel, 2019).

$$\ln Q_e = \ln Q_f + 1/n \ln C_e \quad (12)$$

Experimental data were adapted to Freundlich model and $\ln C_e$ was plotted against $\ln Q_e$.
Q_f and n values were calculated from the cut-off point and slope (Finette et al., 1997; Umpleby et al., 2001).

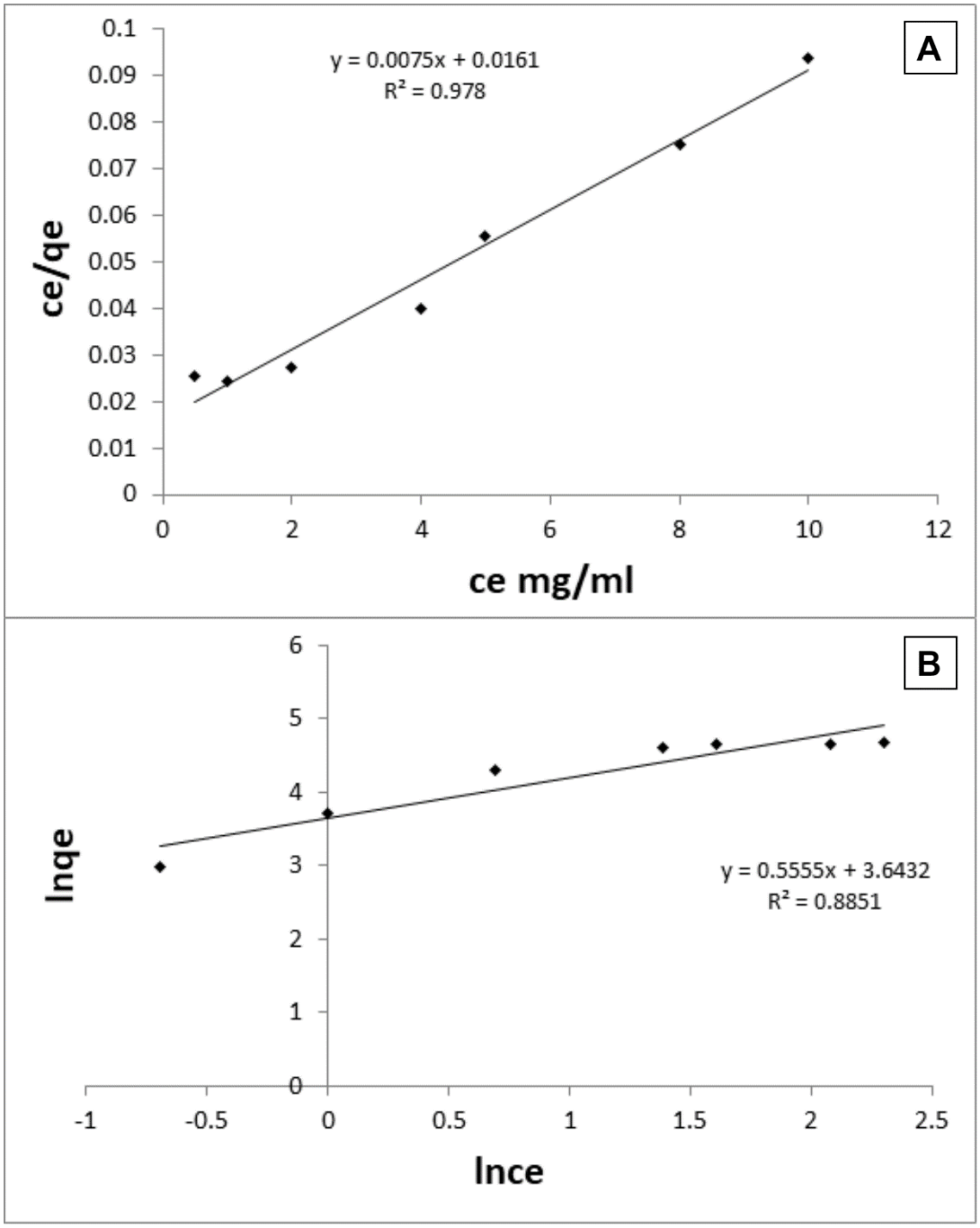

Figure 4.7. Adsorption isotherms. The plot of A) Langmuir and B) Freundlich isotherms.

Figure 4.7 summarizes the both Langmuir and Freundlich adsorption isotherm models. The Q_L, b, Q_F,1/n were calculated the linearization equation and shown in Table 4.3.

Table 4.3. Adsorption Isotherms. Langmuir and Freundlich adsorption isotherm constants for HSA.

Experimental	**Langmuir Constants**			**Freundlich Constants**		
Q_{ex} (mg/g)	Q_L (mg/g)	b (mL/mg)	R^2	Q_F (mg/g)	n	R^2
106.8	133.3	0.47	0.978	38.21	1.80	0.8851

The correlation coefficients R^2 of the Langmuir isotherm obtained as 0.978, which is higher than that of Freundlich (0.8851). The maximum Langmuir (Q_{max}) is adsorption amount was calculated as 133.3, which is closer to experimentally obtained data (106.8) than that of Freundlich. The Freundlich adsorption isotherm constant was found as 1.80 and the Langmuir constants b was ontained as 0.47. The parameters Q_L and Q_F obtained, and the R^2 values showed that the adsorption data is more compatible with Langmuir isotherm, and it can be concluded that the monolayer adsorption is favorable.

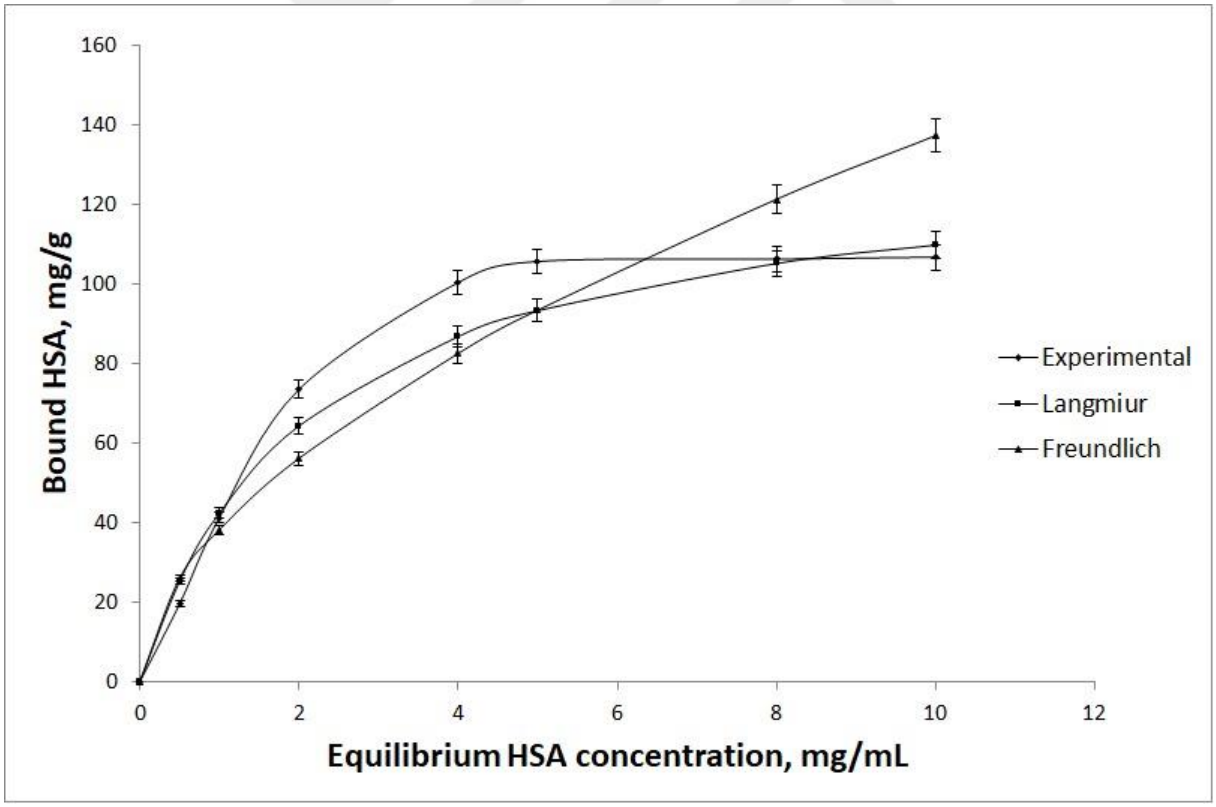

Figure 4.8. Adsorption isotherms. Effect of equilibrium HSA concentration and Langmuir and Freundlich adsorption models. m_{dry}: 0.24 g, V: 10 mL, time: 120 min, pH 7.4, flow rate: 0.5 mL/min, T: 25°C.

The adsorption behavior compatibility also compared in Figure 4.8 by ptotting equilibrium HSA concentration versus Langmuir binding amount, Freundlich binding amount and experimentally binding amount. It is confirmed that the experimental data are in agreement with the Langmuir adsorption model rather than Freundlich adsorption model.

4.3.2. Effect of Interaction Time on HSA Adsorption

In order to evaluate the effect of interaction time on HSA adsorption, the adsorption solution was interacted with HSA-DIP columns for 2 hours and the absorbance value was measured by sampling at certain minutes. After 2 hours, maximum HSA adsorption was reached (see Figure 4.9). The rest of the experiments in this study since, conducted as 2 h and the obtained time depence adsorbed HSA data were used to evaluate binding kinetic evaluations.

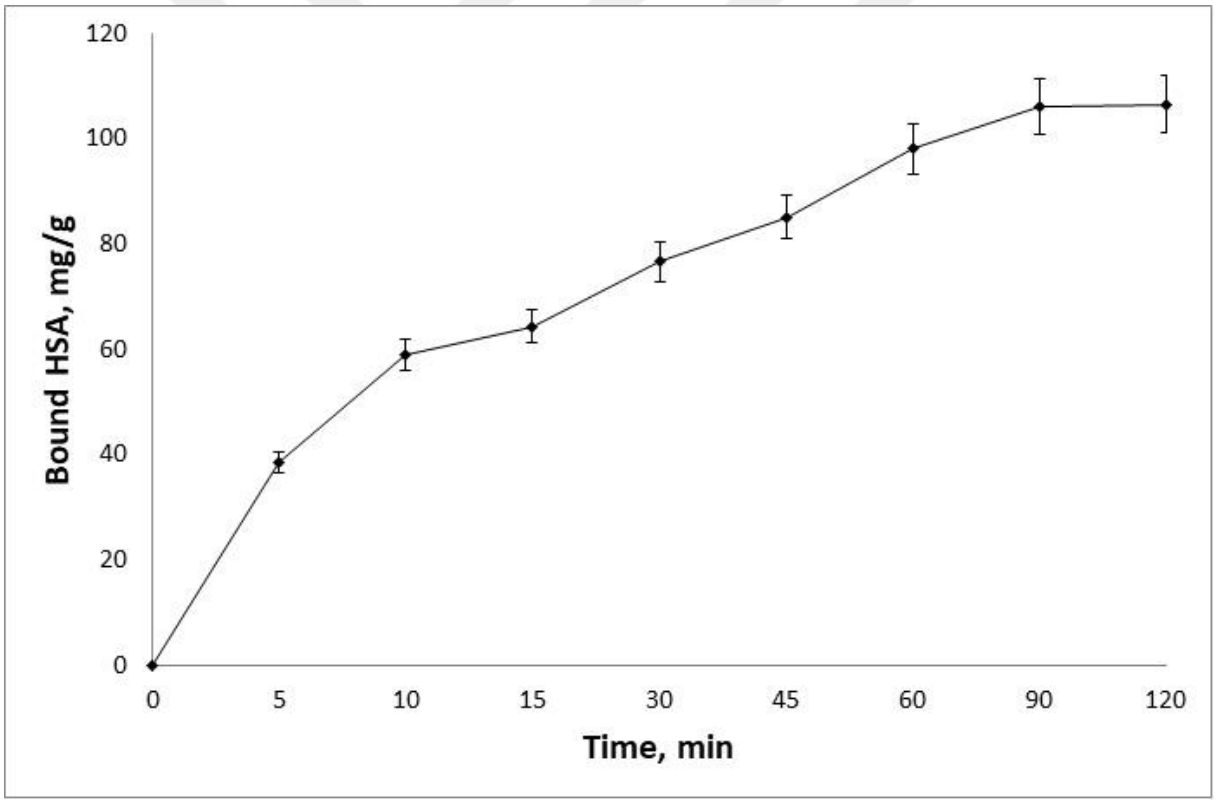

Figure 4.9. Effect of interaction time on HSA adsorption. HSA concentration: 5 mg/mL, m_{dry}: 0.24 g, V: 10 mL, pH 7.4, flow rate: 0.5 mL/min, T: 25°C.

Adsorption kinetics is used to explain the reaction mechanism with the number of molecules bound at the solid-solution interface. It is possible to evaluate the mechanisms controlling the adsorption mechanism (mass transfer, chemical reaction with diffusion control) with the help

of some kinetic models. The experimental time-adsorption amount data were applied to first and second order kinetic models to determine the mechanisms, which control the adsorption process ie. mass transfer or chemical reaction. For the evaluation of the binding mechanism, it is assumed that the HSA concentration in working solution is equal with the HSA concentration on surface of the DIP (Cheung et al., 2001).

The pseudo first-order kinetic model was applied via Lagergren's equation (eq. 1).

$$\Delta q_t/dt = k_1 (q_e - q_t) \quad (13)$$

k_1 is first order adsorption rate constant (min^{-1}); q_e and q_t are HSA adsorption amount at equilibrium and at time t (mg/g), respectively. This equation was linearized as equation 14 and plotted "$\log(q_e-q_t)$" versus "t" to obtain "q_e" and "k_1" from cut-off point and slope

$$\log(q_e - q_t) = \log(q_e) - (k_1 t)/2.303 \quad (14)$$

The pseudo-second order equation expressed as:

$$\Delta q_t /dt = k_2 (q_e - q_t)^2 \quad (15)$$

Here k_2 is pseudo-second order adsorption rate constant (g mg^{-1} min^{-1}). It was linearized as equation 16 and plotted (t/qt) versus "t" to obtain "q_e" and "k_2" from cut-off point and slope;

$$(t/q_t) = (1/k_{2qe}^2) + (1/q_e)\, t \quad (16)$$

Figure 4.10 A and B shows the plots of pseudo first order and second order kinetic models. The k_1, q_e, k_2 values and the correlation coefficients were summarized for comparison in Table 4.4.

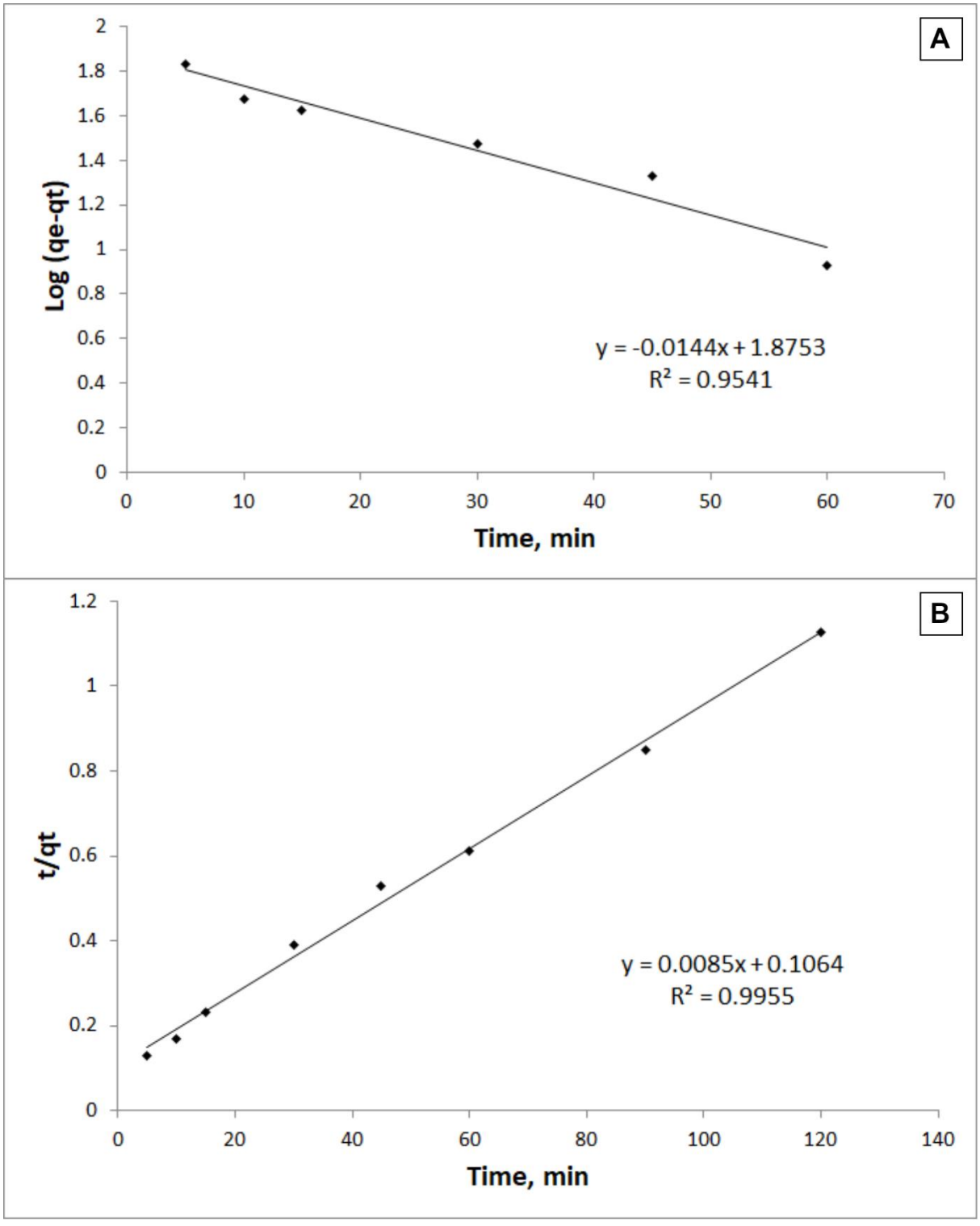

Figure 4.10. Adsorption Kinetics. The plot of A) pseudo first order kinetics and B) pseudo second order kinetics.

Table 4.4. Adsorption Kinetics. Adsorption kinetics model constants and adsorption amounts.

Initial Conc. (mg/mL)	**Exp.**	**Pseudo-first-order-kinetic**			**Pseudo-second-order-kinetic**		
	Q_e (mg/g)	**k_1 (1/dk)**	**q_e (mg/g)**	**R^2**	**k_2 (1/dk)**	**q_e (mg/g)**	**R^2**
5.00	106.8	0.0332	75	0.9541	0.00068	117.647	0.9955

According to results shown in Table 4.4 the adsorption process can be expressed via second order mechanism. Correlation coefficient R^2 is found as 0.9955 for pseudo-second order that is greater than pseudo-first order 0.9541 shows adsorption process controlled by pseudo-second order mechanisms via chemisorption rather than diffusion.

4.3.3. Effect of Flow Rate on HSA Adsorption

For the determination of the effect of flow rate on HSA adsorption property of HSA-DIP columns, flow rate was varied in the range of 0.1-2 mL/min (see Figure 4.11). HSA adsorption amount of HSA-DIP cryogel was observed to decrease dramatically from 118.32 mg/g to 65.87 mg/g as the flow rate was changed between 0.1 to 2 mL/min, respectively. Much better adsorption was achieved at lower flow rates since HSA molecules theoretically have more time for a slow and effective interaction without missing out specific binding regions. Herein, it has been concluded that flow rates of 0.1 mL/min and 0.5 mL/min will be more effective to be employed in the experimental process, with HSA adsorption up 118.32 mg/g and 106.8 mg/g. Even though working with the flow rate of 0.1 mL/min resulted in maximum adsorption within the studied range of flow rate, it would not be effective in terms of time-saving. The flow rate of 1 mL/min and above was time-saving but resulted in much lower HSA adsorption. Therefore, flow rate of 0.5 mL/min was preferred as the optimum flow rate for an effective binding as well as the time-effectiveness.

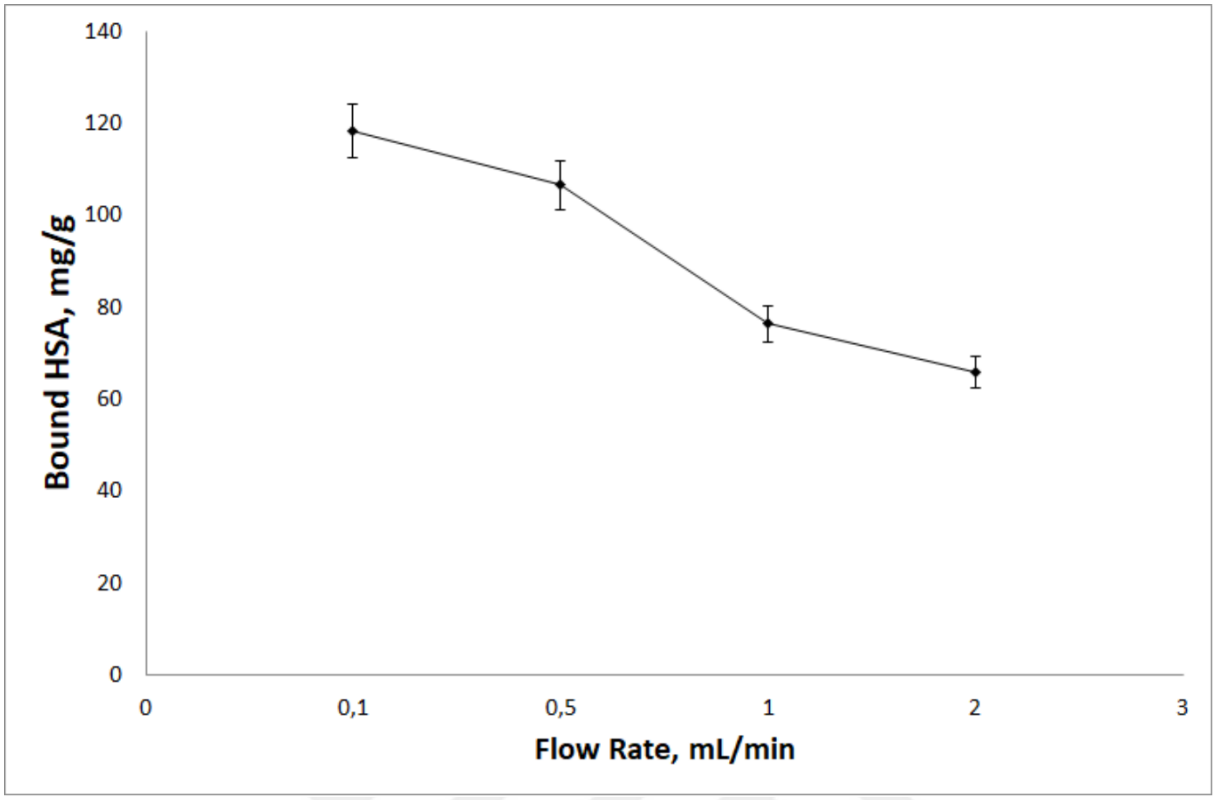

Figure 4.11. Effect of flow rate on HSA adsorption. HSA concentration: 5 mg/mL, m_{dry}: 0.24 g, V: 10 mL, pH 7.4, time: 120 min, T: 25°C.

4.3.4. Effect of Monomer Concentration on HSA Adsorption

The effect of monomer concentration of synthesized cryogels as well as the double-layer imprinted cryogels on maximum HSA adsorption of columns was investigated. It was determined that the adsorption capacity of the HSA-DIP column was much higher than the single layer HSA-imprinted columns (HSA-$MIP_{8\%}$ and HSA-$MIP_{16\%}$), so that the adsorption capacity was significantly increased employing double-layer imprinting technique (see Figure 4.12). The relation between the adsorption capacities and the surface areas of the synthesized columns were also in accordance with the obtained results. Surface areas of HSA-DIP, HSA-$MIP_{16\%}$ and HSA-$MIP_{8\%}$ were found as 39 m^2/g, 21 m^2/g and 12 m^2/g, respectively and it is clear that the adsorption capacities were increased with increasing surface area due to the increase in surface area increased also the effective binding sites. The adsorption capacities were increased with increasing surface area, as expected the increase in surface area increased also the effective binding sites. In this study the amount of specific HSA imprinted cavities increased by increasing surface area of the cryogel columns via second layer construction onto first layer.

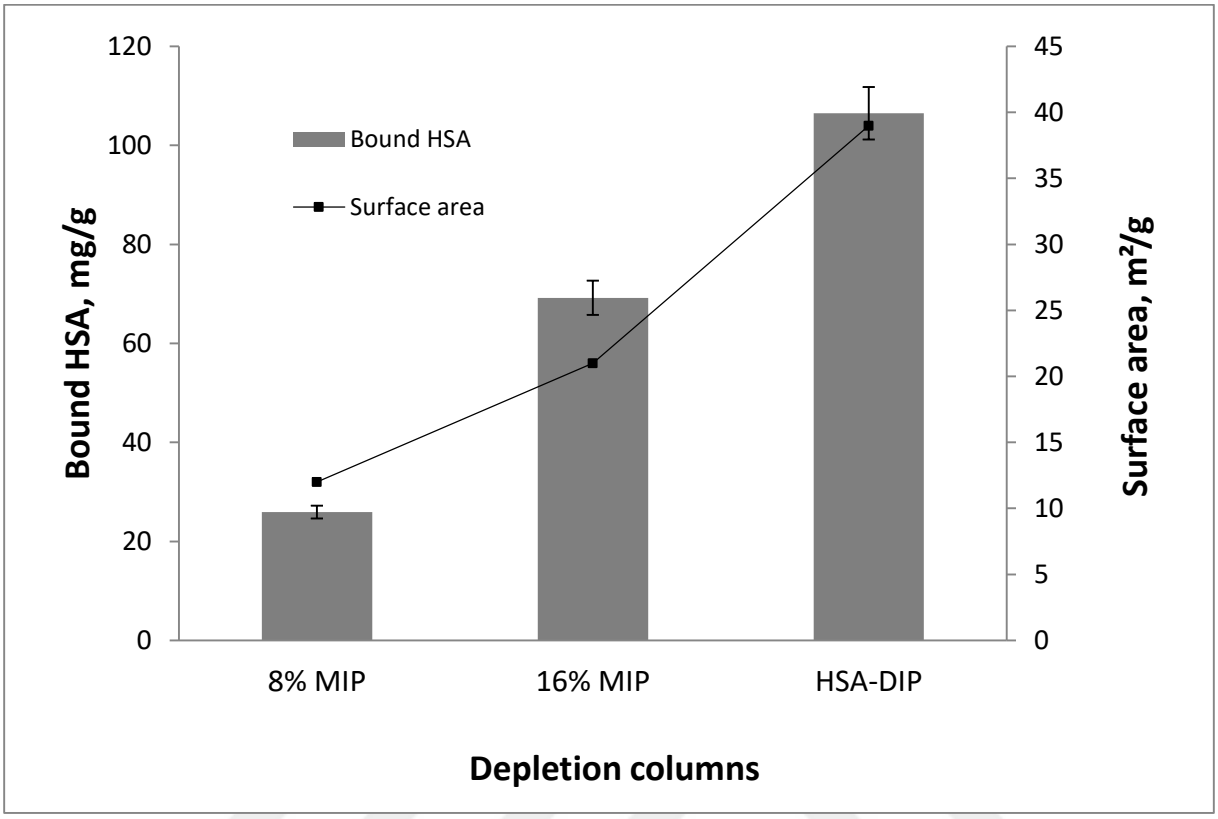

Figure 4.12. Effect of monomer concentration on HSA adsorption. HSA concentration: 5 mg/mL, m_{dry}: 0.24 g, V: 10 mL, pH: 7.4, time: 120 min, flow rate: 0.5 mL/min, T: 25°C.

4.4. Selectivity Studies

Selectivity of HSA-DIP and DL-NIP columns for HSA was evaluated against Hb and IgG as competitor molecule, with two separate analysis of samples: UV spectrophotometry and SDS-PAGE. According to both results, it was concluded that the columns can adsorb HSA quite specifically as compared to competitors.

In order to test selective adsorption property of HSA-DIP, three separate solution of HSA, IgG and Hb was passed through HSA-DIP columns in a continuous system under optimum conditions. 1 mL of sample was taken before and after adsorption for each solution. The concentration of absorbed molecules on HSA-DIP were determined spectrophotometrically at 204 nm, as 53.2 mg/g, 23.4 mg/g and 19.3 mg/g for HSA, IgG and Hb, respectively. The same procedure was applied for DL-NIP columns as the control group and the concentration of adsorbed molecules on DL-NIP was found to be 5.13 mg/g, 13.1 mg/g and 15.5 mg/g for HSA, IgG and Hb, respectively. It was concluded that adsorption capacities of both HSA-DIP and

DL-NIP columns for IgG and Hb, independently, were approximately the same, however, there is a remarkable difference between HSA adsorption capacity of HSA-DIP and that of DL-NIP, in case of HSA. In relation to this, IF values for HSA, IgG and Hb were calculated as 3.42, 2.25, and 1.54, respectively (see Figure 4.13 and Table 4.5).

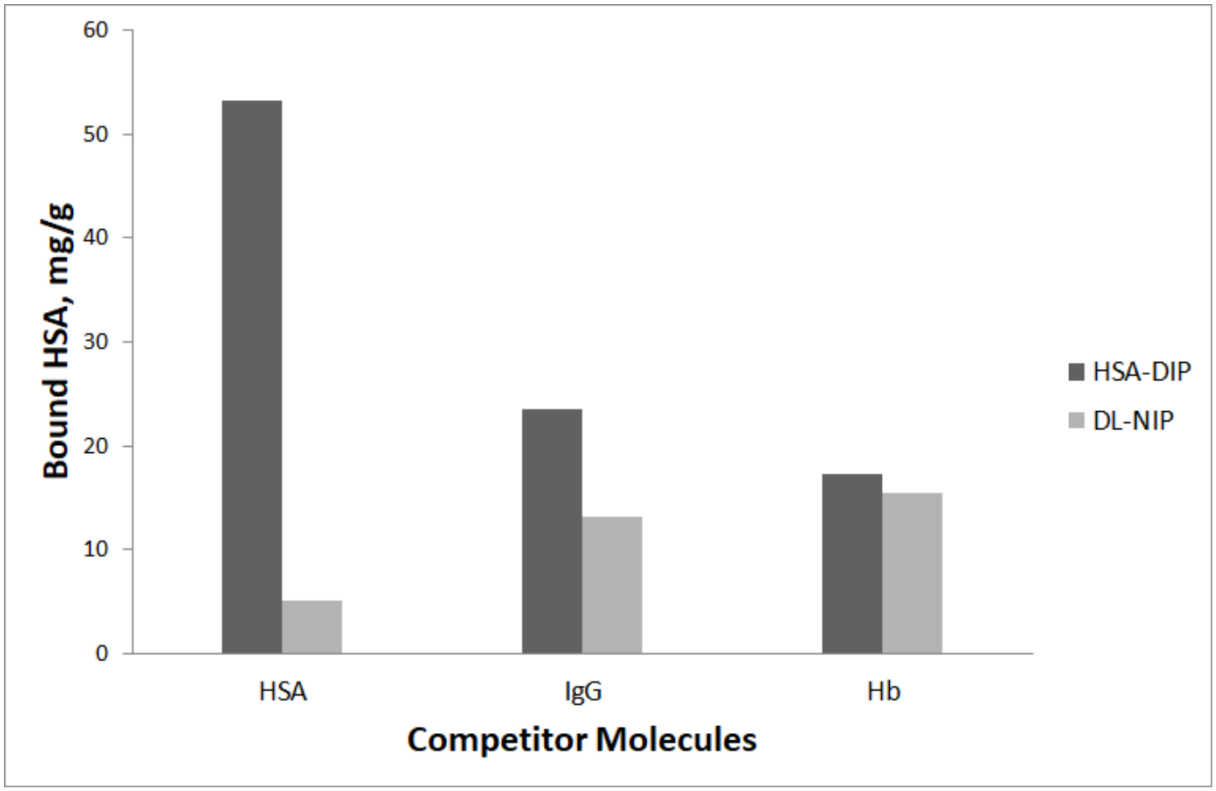

Figure 4.13. Selectivity Studies. Concentrations of each HSA, Hb and IgG solution: 1.5 mg/mL, m_{dry}: 0.24 g, V: 10 mL, pH 7.4, time: 120 min, flow rate: 0.5 mL/min, T: 25°C.

Table 4.5. Selectivity. Selective adsorption properties of synthesized columns for HSA in the presence of competitors.

	HSA-DIP		**DL-NIP**		**IF**	**k**
	Q, mg/g	**Q_d, mL/g**	**Q, mg/g**	**Q_d, mL/g**		
HSA	53.2	32.01	5.13	9.36	3.42	
IgG	23.4	12.59	13.1	5.59	2.25	2.54
Hb	19.3	16.86	15.5	10.92	1.54	1.89

HSA depletion studies from human serum: HSA depletion efficiency of HSA-DIP from human serum was evaluated. The crude HSA concentration was measured as 38 mg/mL. After the interaction with HSA-DIP, the depletion efficacies were increased and calculated as 76%, 80,5%, 93.5%, for 1/1,1/2,1/5 dilution rates, respectively. The elution step was performed after treatment with serum samples, by applying elution solution to HSA-DIP for 2 h. Desorption ratio was achieved as 98 % in elution buffer. The initial and final crude serum samples and elution solution were also applied to SDS-PAGE analysis to show depletion specifically.

4.4.1. SDS-PAGE

A suitable SDS-PAGE protocol was performed, employing the adsorption initial and final samples of HSA-Hb-IgG solution and diluted serum, the desorption solution of adsorption initial solutions, and a proper protein ladder, for further assessment of the selective adsorption properties of synthesized materials. For this purpose, polyacrylamide gel was synthesized with the monomer concentration of 12% (w/v) and a protein ladder within the range of 10-200 kDa was employed, since molecules of interest have molecular weights within this range (HSA: 67 kDa, Hb: 16 kDa x four subunits, IgG: two identical light chains about 25 kDa and two identical heavy chains about 50 kDa). SDS-PAGE gel image is given in Figure 4.14.

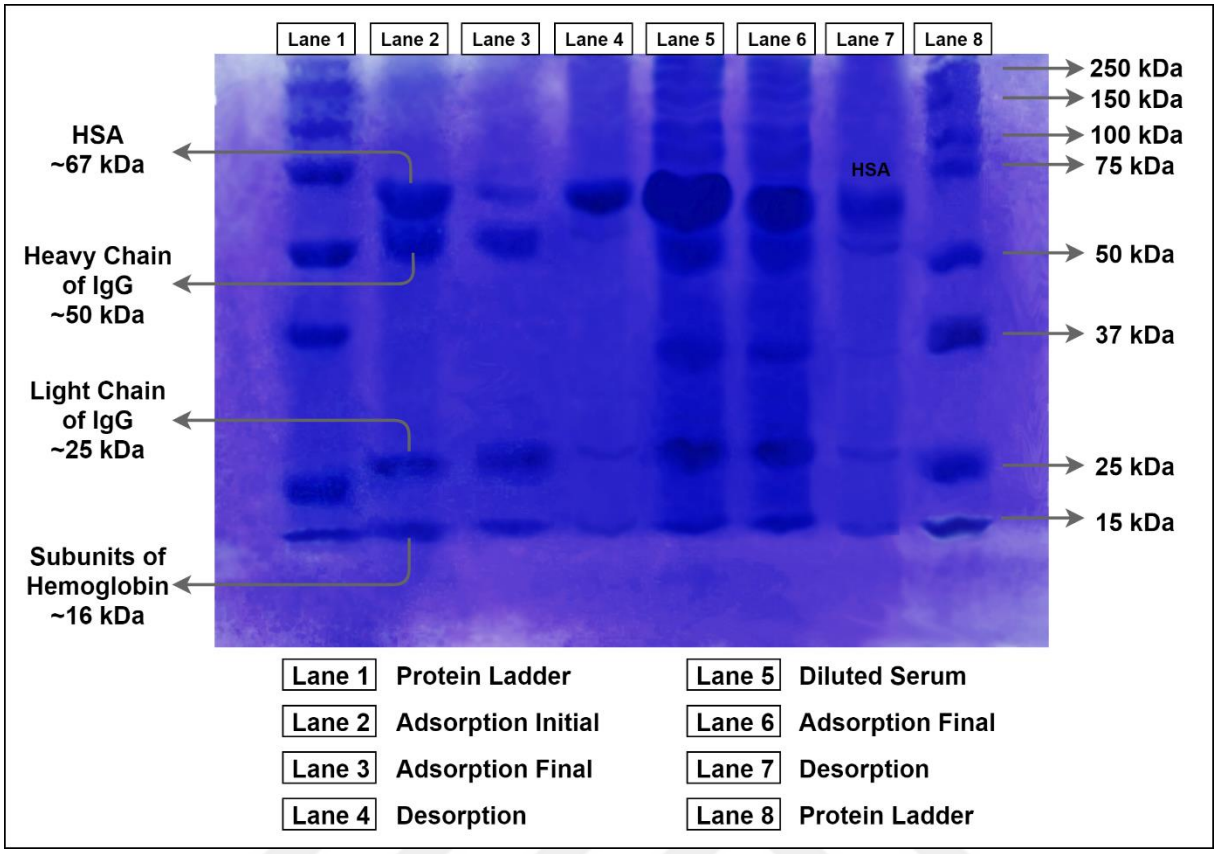

Figure 4.14. SDS-PAGE. Gel image of SDS-PAGE analysis of samples obtained from selectivity studies.

According to SDS-PAGE results, it was clearly observed that HSA-DIP columns can specifically adsorb HSA molecules, in presence of competitor molecules in the adsorption medium. 4 bands were formed in Lane 2 and the presence of HSA, heavy and light chains of IgG, and four identical subunits of Hb was demonstrated utilizing the information provided by Lane 1 and Lane 8 (protein ladders). In Lane 5, multiple intertwined bands were observed due to the complexity of human serum. Adsorption final solutions obtained from HSA-Hb-IgG solution and diluted serum were separately loaded into 3rd and 6th wells and have resulted in the formation of 4 bands in Lane 3 and multiple intertwined bands but with depleted HSA in Lane 6. Obviously decreased HSA concentration and a rather insignificant change in the concentrations of competitors was observed, which was concluded by looking at the band intensity and width. Desorption of adsorbed molecules from separate samples (HSA-Hb-IgG solution in PBS pH 7.4 and diluted serum) have resulted in a single intense band corresponding to HSA and slight bands corresponding to competitors in Lane 4 and Lane 7. In the light of these results, the success of the study in terms of selectivity have been fully confirmed.

4.5. Desorption and Reusability Studies

The reusability of HSA-DIP columns was tested by repeated adsorption-desorption experiments, and it was concluded that there was no significant decrease in the adsorption capacity of the columns after 10 adsorption-desorption cycles (see Figure 4.15).

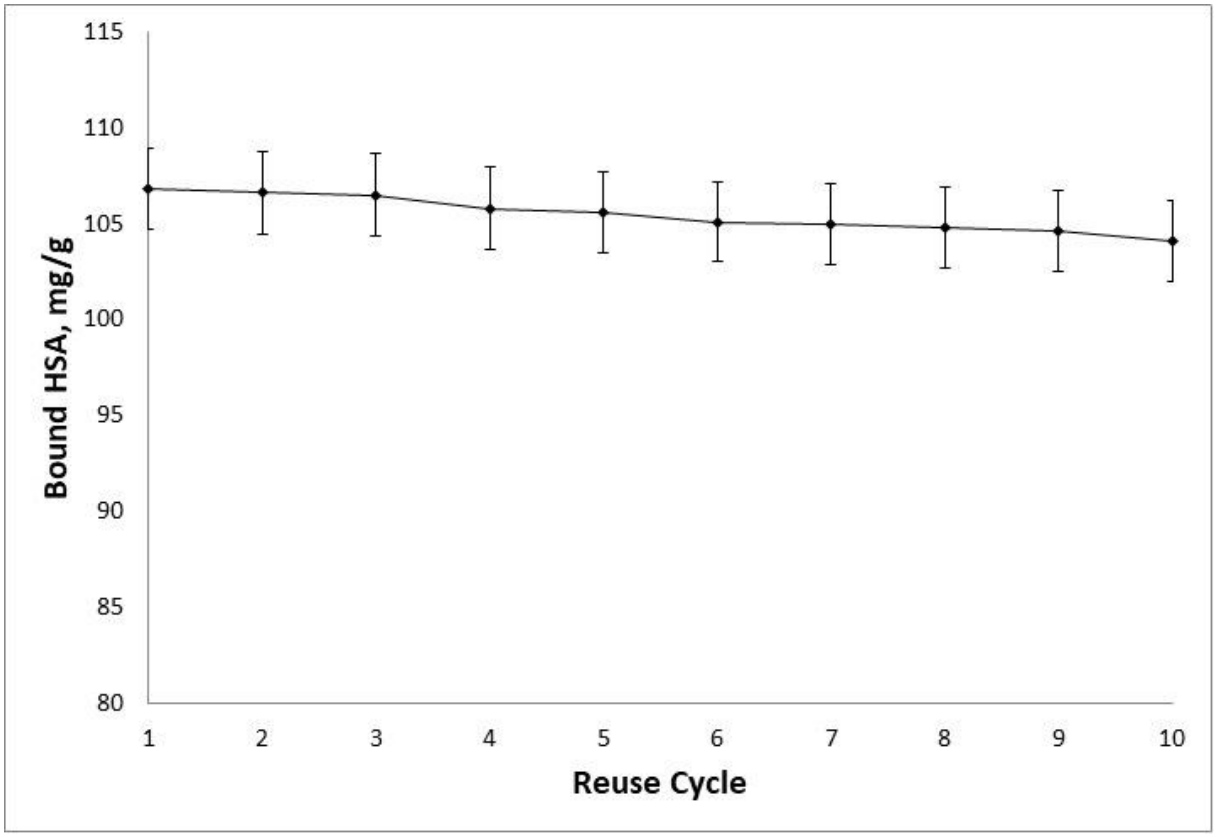

Figure 4.15. Reusability Studies. Equilibrium HSA concentration: 5 mg/mL, m_{dry}: 0.24 g, V: 10 mL, pH 7.4, time: 120 min, flow rate: 0.5 mL/min, T: 25°C.

5. CONCLUSIONS

In this thesis study, brand new HSA double-imprinted biocompatible spongy cryogels which provide specific depletion of HSA in one step with high binding capacities were synthesized using a novel methodology: double-layer imprinting technique. Thus, a sensitive, fast and cost-effective material was developed for quantitative analysis of HSA directly from human serum. Synthesized polymers were analyzed morphologically and tested in terms of adsorption properties, selectivity for HSA and reusability. The water uptake ratios were calculated as 84% for HSA-DIP, 82% for DL-NIP, 89% for HSA-$MIP_{8\%}$ and 88% for HSA-$MIP_{16\%}$. Surface areas of HSA-DIP, DL-NIP, HSA-$MIP_{16\%}$ and HSA-$MIP_{8\%}$ were found to be 39 m^2/g, 37m^2/g, 21 m^2/g and 12 m^2/g, respectively. Maximum HSA adsorption of HSA-DIP and DL-NIP was calculated as 106.8 mg/g and 5.14 mg/g, respectively. Spectrophotometric measurements and SDS-PAGE analysis have demonstrated that HSA-DIPs has an excellent selectivity for HSA as compared to competitors (Hb and IgG). Repeated adsorption-desorption cycles have showed that HSA-DIP can be used up to 10 times without any significant decrease in selective HSA adsorption capacity. The reason this study will have an impact is not only because of the use of a novel imprinting technique that has not been studied before in literature, but also the fact that the obtained results within the scope of the study are comparable to the studies in the literature.

REFERENCES

Alexander, C., Andersson, H. S., Andersson, L. I., Ansell, R. J., Kirsch, N., Nicholls, I. A., ... & Whitcombe, M. J. (2006). Molecular imprinting science and technology: a survey of the literature for the years up to and including 2003. *Journal of Molecular Recognition: An Interdisciplinary Journal*, *19*(2), 106-180.

Ali, M., & Mahmud, H. B. (2015, March). The effects of concentration and salinity on polymer adsorption isotherm at sandstone rock surface. In IOP Conference Series: *Materials Science and Engineering* (Vol. 78, No. 1, p. 012038). IOP Publishing.

Altıntaş, E. B., Tüzmen, N., Uzun, L., & Denizli, A. (2007). Immobilized metal affinity adsorption for antibody depletion from human serum with monosize beads. *Industrial & engineering chemistry research*, *46*(23), 7802-7810.

Andaç, M. (2015). Cibacron blue immobilized poly (glycidyl-methacrylate) nanobeads for albumin removal in proteome studies. *Artificial cells, nanomedicine, and biotechnology*, *43*(2), 133-139.

Andaç, M., Baydemir, G., Yavuz, H., & Denizli, A. (2012b). Molecularly imprinted composite cryogel for albumin depletion from human serum. *Journal of Molecular Recognition*, *25*(11), 555-563.

Andaç, M., Galaev, I. Y., & Denizli, A. (2013). Molecularly imprinted poly (hydroxyethyl methacrylate) based cryogel for albumin depletion from human serum. *Colloids and Surfaces B: Biointerfaces*, *109*, 259-265.

Andac, M., Galaev, I., & Denizli, A. (2012a). Dye attached poly (hydroxyethyl methacrylate) cryogel for albumin depletion from human serum. *Journal of separation science*, *35*(9), 1173-1182.

Andersson, L. I. (2000). Molecular imprinting: developments and applications in the analytical chemistry field. *Journal of Chromatography B: Biomedical Sciences and Applications*, *745*(1), 3-13.

Arshady, R., & Mosbach, K. (1981). Synthesis of substrate-selective polymers by host-guest polymerization. *Die Makromolekulare Chemie: Macromolecular Chemistry and Physics*, *182*(2), 687-692.

Asliyuce, S., Uzun, L., Say, R., & Denizli, A. (2013). Immunoglobulin G recognition with Fab fragments imprinted monolithic cryogels: evaluation of the effects of metal-ion assisted-coordination of template molecule. *Reactive and Functional Polymers*, *73*(6), 813-820.

Bat, E. (2016). Hydroxyethyl methacrylate based nanocomposite hydrogels with tunable pore architecture. *Journal of the Turkish Chemical Society Section A: Chemistry*, *3*(3), 607-622.

Baydemir, G., & Denizli, A. (2015). Heparin removal from human plasma using molecular imprinted cryogels. *Artificial Cells, Nanomedicine, and Biotechnology*, *43*(6), 403-412.

Bereli, N., Şener, G., Altıntaş, E. B., Yavuz, H., & Denizli, A. (2010). Poly (glycidyl methacrylate) beads embedded cryogels for pseudo-specific affinity depletion of albumin and immunoglobulin G. *Materials Science and Engineering: C*, *30*(2), 323-329.

Bergmann, N. M., & Peppas, N. A. (2008). Molecularly imprinted polymers with specific recognition for macromolecules and proteins. *Progress in Polymer Science*, *33*(3), 271-288.

Braun, N., Erley, C., Klein, R., Kötter, I., Saal, J., & Risler, T. (2000). Immunoadsorption onto protein A induces remission in severe systemic lupus erythematosus. *Nephrology Dialysis Transplantation*, *15*(9), 1367-1372.

Caironi, P., & Gattinoni, L. (2009). The clinical use of albumin: the point of view of a specialist in intensive care. *Blood Transfusion*, *7*(4), 259.

Chen, L., Xu, S., & Li, J. (2011). Recent advances in molecular imprinting technology: current status, challenges and highlighted applications. *Chemical Society Reviews*, *40*(5), 2922-2942.

Cheung, C. W., Porter, J. F., & McKay, G. (2001). Sorption kinetic analysis for the removal of cadmium ions from effluents using bone char. *Water research*, *35*(3), 605-612.

Dainiak, M. B., Galaev, I. Y., Kumar, A., Plieva, F. M., & Mattiasson, B. (2007). Chromatography of living cells using supermacroporous hydrogels, cryogels. *Cell Separation*, 101-127.

Daniel, S., Babu, P. E., & Rao, T. P. (2005). Preconcentrative separation of palladium (II) using palladium (II) ion-imprinted polymer particles formed with different quinoline derivatives and evaluation of binding parameters based on adsorption isotherm models. *Talanta*, *65*(2), 441-452.

de Jesus, J. R., da Silva Fernandes, R., de Souza Pessôa, G., Raimundo Jr, I. M., & Arruda, M. A. Z. (2017). Depleting high-abundant and enriching low-abundant proteins in human serum: an evaluation of sample preparation methods using magnetic nanoparticle, chemical depletion and immunoaffinity techniques. *Talanta*, *170*, 199-209.

Denizli, A., Tuncel, A., Kozluca, A., Ecevit, K., & Pişkin, E. (1997). Cibacron blue F3G-A attached poly (vinyl alcohol) particles for specific albumin adsorption. *Separation science and technology*, *32*(5), 1003-1015.

Ersöz, A., Say, R., & Denizli, A. (2004). Ni (II) ion-imprinted solid-phase extraction and preconcentration in aqueous solutions by packed-bed columns. *Analytica Chimica Acta*, *502*(1), 91-97.

Ertürk, G., & Mattiasson, B. (2017). Molecular imprinting techniques used for the preparation of biosensors. *Sensors*, *17*(2), 288.

Fanali, G., Di Masi, A., Trezza, V., Marino, M., Fasano, M., & Ascenzi, P. (2012). Human serum albumin: from bench to bedside. *Molecular aspects of medicine*, *33*(3), 209-290.

Finette, G. M., Mao, Q. M., & Hearn, M. T. (1997). Comparative studies on the isothermal characteristics of proteins adsorbed under batch equilibrium conditions to ion-exchange, immobilised metal ion affinity and dye affinity matrices with different ionic strength and temperature conditions. *Journal of Chromatography A*, *763*(1-2), 71-90.

Fu, X., Yang, Q., Zhou, Q., Lin, Q., & Wang, C. (2015). Template-monomer interaction in molecular imprinting: is the strongest the best?. *Open Journal of Organic Polymer Materials*, *5*(02), 58.

Gao, F. X., Zhao, X. L., He, X. W., Li, W. Y., & Zhang, Y. K. (2013). A pH and temperature dual-responsive macroporous molecularly imprinted cryogel for enhanced recognition capability towards ovalbumin. *Analytical Methods*, *5*(23), 6700-6708.

Garcia-Martinez, R., Noiret, L., Sen, S., Mookerjee, R., & Jalan, R. (2015). Albumin infusion improves renal blood flow autoregulation in patients with acute decompensation of cirrhosis and acute kidney injury. *Liver International*, *35*(2), 335-343.

Garipcan, B., & Denizli, A. (2002). A novel affinity support material for the separation of immunoglobulin G from human plasma. *Macromolecular Bioscience*, *2*(3), 135-144.

Garipcan, B., Andaç, M., Uzun, L., & Denizli, A. (2004). Methacryloylamidocysteine functionalized poly (2-hydroxyethyl methacrylate) beads and its design as a metal-chelate affinity support for human serum albumin adsorption. *Reactive and Functional Polymers*, *59*(2), 119-128.

Gelamo, E. L., Silva, C. H. T. P., Imasato, H., & Tabak, M. (2002). Interaction of bovine (BSA) and human (HSA) serum albumins with ionic surfactants: spectroscopy and modelling. *Biochimica et Biophysica Acta (BBA)-Protein Structure and Molecular Enzymology*, *1594*(1), 84-99.

Gökay, Ö., Karakoc, V., Andaç, M., Türkmen, D., & Denizli, A. (2015). Dye-attached magnetic poly (hydroxyethyl methacrylate) nanospheres for albumin depletion from human plasma. *Artificial cells, nanomedicine, and biotechnology*, *43*(1), 62-70.

Govorukhina, N. I., Keizer-Gunnink, A., Van der Zee, A. G. J., De Jong, S., De Bruijn, H. W. A., & Bischoff, R. (2003). Sample preparation of human serum for the analysis of tumor markers: Comparison of different approaches for albumin and γ-globulin depletion. *Journal of Chromatography A*, *1009*(1-2), 171-178.

Guizado, T. C. (2014). Analysis of the structure and dynamics of human serum albumin. *Journal of molecular modeling*, *20*(10), 2450.

Gun'ko, V. M., Savina, I. N., & Mikhalovsky, S. V. (2013). Cryogels: morphological, structural and adsorption characterisation. *Advances in colloid and interface science*, *187*, 1-46.

Guo, Y., Chen, Y., Zhu, X., Pan, Z., Zhang, X., Wang, J., & Fu, N. (2018). Self-assembled nanosensor based on squaraine dye for specific recognition and detection of human serum albumin. *Sensors and Actuators B: Chemical*, *255*, 977-985.

Hajizadeh, S., Xu, C., Kirsebom, H., Ye, L., & Mattiasson, B. (2013). Cryogelation of molecularly imprinted nanoparticles: A macroporous structure as affinity chromatography column for removal of β-blockers from complex samples. *Journal of Chromatography A*, *1274*, 6-12.

Hansen, D. E. (2007). Recent developments in the molecular imprinting of proteins. *Biomaterials*, *28*(29), 4178-4191.

Hawkins, J. W., & Dugaiczyk, A. (1982). The human serum albumin gene: structure of a unique locus. *Gene*, *19*(1), 55-58.

Heli, H., Sattarahmady, N., Jabbari, A., Moosavi-Movahedi, A. A., Hakimelahi, G. H., & Tsai, F. Y. (2007). Adsorption of human serum albumin onto glassy carbon surface–Applied to albumin-modified electrode: Mode of protein–ligand interactions. *Journal of Electroanalytical Chemistry*, *610*(1), 67-74.

Hillberg, A. L., & Tabrizian, M. (2008). Biomolecule imprinting: Developments in mimicking dynamic natural recognition systems. *Irbm*, *29*(2-3), 89-104.

Hoshino, Y., Kodama, T., Okahata, Y., & Shea, K. J. (2008). Peptide imprinted polymer nanoparticles: a plastic antibody. *Journal of the American Chemical Society*, *130*(46), 15242-15243.

Hu, C. H., & Chou, T. C. (2009). Albumin molecularly imprinted polymer prepared with a semi-rigid crosslinker in mixed organic/aqueous media. *Microchimica Acta*, *165*(3), 399-405.

Hu, S., Loo, J. A., & Wong, D. T. (2006). Human body fluid proteome analysis. *Proteomics*, *6*(23), 6326-6353.

Huang, S., Li, F., Liao, C., Zheng, B., Du, J., & Xiao, D. (2017). A selective and sensitive fluorescent probe for the determination of HSA and trypsin. *Talanta*, *170*, 562-568.

Hülshoff, A., Schricker, T., Elgendy, H., Hatzakorzian, R., & Lattermann, R. (2013). Albumin synthesis in surgical patients. *Nutrition*, *29*(5), 703-707.

Image of RCSB PDB (rcsb.org) of 1AO6 (S. Sugio, A. Kashima, S. Mochizuki, M. Noda, K. Kobayashi (1999) Crystal structure of human serum albumin at 2.5 Å resolution, Protein Engineering, Design and Selection, 12:6, 439-446) created with The PyMOL Molecular Graphics System, Version 2.0 Schrödinger, LLC.

Jacobs, J. M., Adkins, J. N., Qian, W. J., Liu, T., Shen, Y., Camp, D. G., & Smith, R. D. (2005). Utilizing human blood plasma for proteomic biomarker discovery. *Journal of proteome research*, *4*(4), 1073-1085.

Jia, M., Zhang, Z., Li, J., Ma, X., Chen, L., & Yang, X. (2018). Molecular imprinting technology for microorganism analysis. *TrAC Trends in Analytical Chemistry*, *106*, 190-201.

Kartal, F., & Denizli, A. (2014). Surface molecularly imprinted magnetic microspheres for the recognition of albumin. *Journal of separation science*, *37*(15), 2077-2086.

Koohpaei, A. R., Shahtaheri, S. J., Ganjali, M. R., Forushani, A. R., & Golbabaei, F. (2008). Application of multivariate analysis to the screening of molecularly imprinted polymers (MIPs) for ametryn. *Talanta*, *75*(4), 978-986.

Koutroukides, T. A., Jaros, J. A., Amess, B., Martins-de-Souza, D., Guest, P. C., Rahmoune, H., ... & Lilley, K. S. (2013). Identification of protein biomarkers in human serum using iTRAQ and shotgun mass spectrometry. In *Immunoproteomics* (pp. 291-307). Humana Press, Totowa, NJ.

Kumar, A., & Srivastava, A. (2010). Cell separation using cryogel-based affinity chromatography. *Nature protocols*, *5*(11), 1737-1747.

Labrou, N. E., & Clonis, Y. D. (1995). The interaction of Candida boidinii formate dehydrogenase with a new family of chimeric biomimetic dye-ligands. *Archives of biochemistry and biophysics*, *316*(1), 169-178.

Lee, P., & Wu, X. (2015). Modifications of human serum albumin and their binding effect. *Current pharmaceutical design*, *21*(14), 1862-1865.

Liu, J., Deng, Q., Tao, D., Yang, K., Zhang, L., Liang, Z., & Zhang, Y. (2014). Preparation of protein imprinted materials by hierarchical imprinting techniques and application in selective depletion of albumin from human serum. *Scientific reports*, *4*, 5487.

Lozinsky, V. I., & Plieva, F. M. (1998). Poly (vinyl alcohol) cryogels employed as matrices for cell immobilization. 3. Overview of recent research and developments. *Enzyme and microbial technology*, *23*(3-4), 227-242.

Lozinsky, V. I., Galaev, I. Y., Plieva, F. M., Savina, I. N., Jungvid, H., & Mattiasson, B. (2003). Polymeric cryogels as promising materials of biotechnological interest. *TRENDS in Biotechnology*, *21*(10), 445-451.

Ma, X. T., He, X. W., Li, W. Y., & Zhang, Y. K. (2017). Epitope molecularly imprinted polymer coated quartz crystal microbalance sensor for the determination of human serum albumin. *Sensors and Actuators B: Chemical*, *246*, 879-886.

Ma, Z. Y., Guan, Y. P., & Liu, H. Z. (2005). Synthesis of monodisperse nonporous crosslinked poly (glycidyl methacrylate) particles with metal affinity ligands for protein adsorption. *Polymer international*, *54*(11), 1502-1507.

Majoor, C. L. H. (1978). Serum albumin in clinical practice: A historical review. In *Clinical Aspects of Albumin* (pp. 97-116). Springer, Dordrecht.

Martín-Esteban, A. (2013). Molecularly-imprinted polymers as a versatile, highly selective tool in sample preparation. *TrAC Trends in Analytical Chemistry*, *45*, 169-181.

Martínez-Vertel, J. J., Villaquirán-Vargas, A. P., Villar-García, Á., Moreno-Díaz, D. F., & Rodríguez-Castelblanco, A. X. (2019). Polymer adsorption isotherms with NaCl and CaCl 2 on kaolinite substrates. *Dyna*, *86*(210), 66-73.

Mattiasson, B., Kumar, A., & Galeaev, I. Y. (Eds.). (2009). *Macroporous polymers: production properties and biotechnological/biomedical applications*. CRC Press.

McCallum, M. M., Pawlak, A. J., Shadrick, W. R., Simeonov, A., Jadhav, A., Yasgar, A., ... & Arnold, L. A. (2014). A fluorescence-based high throughput assay for the determination of small molecule− human serum albumin protein binding. *Analytical and bioanalytical chemistry*, *406*(7), 1867-1875.

Merlot, A. M., Kalinowski, D. S., & Richardson, D. R. (2014). Unraveling the mysteries of serum albumin—more than just a serum protein, ‖ Front.

Minchiotti, L., Galliano, M., Kragh-Hansen, U., & Peters Jr, T. (2008). Mutations and polymorphisms of the gene of the major human blood protein, serum albumin. *Human mutation*, *29*(8), 1007-1016.

Moreno-Bondi, M. C., Navarro-Villoslada, F., Benito-Peña, E., & Urraca, J. L. (2008). Molecularly imprinted polymers as selective recognition elements in optical sensing. *Current Analytical Chemistry*, *4*(4), 316-340.

Mosbach, K., & Ramström, O. (1996). The emerging technique of molecular imprinting and its future impact on biotechnology. *Bio/technology*, *14*(2), 163-170.

Odabaşı, M., & Denizli, A. (2004). Cibacron Blue F3GA-attached magnetic poly (2-hydroxyethyl methacrylate) beads for human serum albumin adsorption. *Polymer international*, *53*(3), 332-338.

Odabaşı, M., Say, R., & Denizli, A. (2007). Molecular imprinted particles for lysozyme purification. *Materials Science and Engineering: C*, *27*(1), 90-99.

Okay, O., & Lozinsky, V. I. (2014). Synthesis and structure–property relationships of cryogels. In *Polymeric Cryogels* (pp. 103-157). Springer, Cham.

Ozmen, M. M., & Okay, O. (2005). Superfast responsive ionic hydrogels with controllable pore size. *Polymer*, *46*(19), 8119-8127.

Peters Jr, T. (1995). *All about albumin: biochemistry, genetics, and medical applications*. Academic press.

Piletsky, S., Canfarotta, F., Poma, A., Bossi, A. M., & Piletsky, S. (2020). Molecularly imprinted polymers for cell recognition. *Trends in biotechnology*, *38*(4), 368-387.

Plieva, F. M., Karlsson, M., Aguilar, M. R., Gomez, D., Mikhalovsky, S., & Galaev, I. Y. (2005). Pore structure in supermacroporous polyacrylamide based cryogels. *Soft Matter*, *1*(4), 303-309.

Reichelt, S., Becher, J., Weisser, J., Prager, A., Decker, U., Möller, S., ... & Schnabelrauch, M. (2014). Biocompatible polysaccharide-based cryogels. *Materials Science and Engineering: C*, *35*, 164-170.

Resmini, M. (2012). Molecularly imprinted polymers as biomimetic catalysts. *Analytical and bioanalytical chemistry*, *402*(10), 3021-3026.

Say, R., Birlik, E., Ersöz, A., Yılmaz, F., Gedikbey, T., & Denizli, A. (2003). Preconcentration of copper on ion-selective imprinted polymer microbeads. *Analytica Chimica Acta*, *480*(2), 251-258.

Schalich, K. M., Herren, A. W., & Selvaraj, V. (2020). Analysis of differential strategies to enhance detection of low-abundance proteins in the bovine serum proteome. *Animal Science Journal*, *91*(1), e13388.

Schirhagl, R., Podlipna, D., Lieberzeit, P. A., & Dickert, F. L. (2010). Comparing biomimetic and biological receptors for insulin sensing. *Chemical communications*, *46*(18), 3128-3130.

Shamsipur, M., Fasihi, J., Khanchi, A., Hassani, R., Alizadeh, K., & Shamsipur, H. (2007). A stoichiometric imprinted chelating resin for selective recognition of copper (II) ions in aqueous media. *Analytica chimica acta*, *599*(2), 294-301.

Sharma, P. S., Pietrzyk-Le, A., D'souza, F., & Kutner, W. (2012). Electrochemically synthesized polymers in molecular imprinting for chemical sensing. *Analytical and bioanalytical chemistry*, *402*(10), 3177-3204.

Singabraya, D., Bultel, L., Siñeriz, F., Mothéré, M., Lesur, D., Kovensky, J., & Papy-Garcia, D. (2012). Molecular imprinting technology for specific recognition of heparan sulfate like disaccharides. *Talanta*, *99*, 833-839.

Singh, P., Mittal, L. S., Kaur, S., Kaur, S., Bhargava, G., & Kumar, S. (2018). Self-assembled small molecule based fluorescent detection of serum albumin proteins: Clinical detection and cell imaging. *Sensors and Actuators B: Chemical*, *255*, 478-489.

Steinhardt, J., Krijn, J., & Leidy, J. G. (1971). Differences between bovine and human serum albumins. Binding isotherms, optical rotatory dispersion, viscosity, hydrogen ion titration, and fluorescence effects. *Biochemistry*, *10*(22), 4005-4015.

Sugio, S., Kashima, A., Mochizuki, S., Noda, M., & Kobayashi, K. (1999). Crystal structure of human serum albumin at 2.5 Å resolution. *Protein engineering*, *12*(6), 439-446.

Suwinski, R., Giglok, M., Galwas-Kliber, K., Idasiak, A., Jochymek, B., Deja, R., ... & Butkiewicz, D. (2019). Blood serum proteins as biomarkers for prediction of survival, locoregional control and distant metastasis rate in radiotherapy and radio-chemotherapy for non-small cell lung cancer. *BMC cancer*, *19*(1), 427.

Tamahkar, E., Babaç, C., Kutsal, T., Pişkin, E., & Denizli, A. (2010). Bacterial cellulose nanofibers for albumin depletion from human serum. *Process Biochemistry*, *45*(10), 1713-1719.

Tamahkar, E., Bereli, N., Say, R., & Denizli, A. (2011). Molecularly imprinted supermacroporous cryogels for cytochrome c recognition. *Journal of separation science*, *34*(23), 3433-3440.

Tan, C. J., & Tong, Y. W. (2007). Molecularly imprinted beads by surface imprinting. *Analytical and bioanalytical chemistry*, *389*(2), 369-376.

Tsukagoshi, K., Murata, M., Maeda, M., & Dhal, P. (2001). In molecularly imprinted polymers: man-made mimics of antibodies and their applications in analytical chemistry. *Techniques and instrumentation in analytical chemistry*, *23*, 245-269.

Tuncel, A., Denizli, A., Purvis, D., Lowe, C. R., & Pişkin, E. (1993). Cibacron Blue F3G-A-attached monosize poly (vinyl alcohol)-coated polystyrene microspheres for specific albumin adsorption. *Journal of Chromatography A*, *634*(2), 161-168.

Umpleby, R. J., Baxter, S. C., Chen, Y., Shah, R. N., & Shimizu, K. D. (2001). Characterization of MIPs using heterogeneous binding models. *Anal Chem*, *73*, 4584-4591.

Uzun, L., Armutcu, C., Biçen, Ö., Ersöz, A., Say, R., & Denizli, A. (2013). Simultaneous depletion of immunoglobulin G and albumin from human plasma using novel monolithic cryogel columns. *Colloids and Surfaces B: Biointerfaces*, *112*, 1-8.

Vasapollo, G., Sole, R. D., Mergola, L., Lazzoi, M. R., Scardino, A., Scorrano, S., & Mele, G. (2011). Molecularly imprinted polymers: present and future prospective. *International journal of molecular sciences*, *12*(9), 5908-5945.

Verheyen, E. (2011). *From imprinting efforts to new concepts in controlled release of proteins* (Doctoral dissertation, Utrecht University).

Wang, Z. M., Ho, J. X., Ruble, J. R., Rose, J., Rüker, F., Ellenburg, M., ... & Carter, D. C. (2013). Structural studies of several clinically important oncology drugs in complex with human serum albumin. *Biochimica et Biophysica Acta (BBA)-General Subjects*, *1830*(12), 5356-5374.

Wulff, G., & Sarhan, A. (1972). Über die Anwendung von enzymanalog gebauten Polymeren zur Racemattrennung. *Angewandte Chemie*, *84*(8), 364-364.

Yan, H., & Row, K. H. (2006). Characteristic and synthetic approach of molecularly imprinted polymer. *International journal of molecular Sciences*, *7*(5), 155-178.

Yao, K., Shen, S., Yun, J., Wang, L., Chen, F., & Yu, X. (2007). Protein adsorption in supermacroporous cryogels with embedded nanoparticles. *Biochemical engineering journal*, *36*(2), 139-146.

Ye, L., Cormack, P. A., & Mosbach, K. (1999). Molecularly imprinted monodisperse microspheres for competitive radioassay. *Analytical Communications*, *36*(2), 35-38.

Yıldırım, M., & Peşint, G. B. (2020). Molecularly imprinted spongy columns for Angiotensin (II) recognition from human serum. *Biotechnology progress*.

Zhang, H., Song, T., Zong, F., Chen, T., & Pan, C. (2008). Synthesis and characterization of molecularly imprinted polymers for phenoxyacetic acids. *International journal of molecular sciences*, *9*(1), 98-106.

Zhang, Y., Guo, Y., Xianyu, Y., Chen, W., Zhao, Y., & Jiang, X. (2013). Nanomaterials for ultrasensitive protein detection. *Advanced Materials*, *25*(28), 3802-3819.

Zink, S., Moura, F. A., da Silva Autreto, P. A., Galvao, D. S., & Mizaikoff, B. (2018). Efficient prediction of suitable functional monomers for molecular imprinting via local density of states calculations. *Physical Chemistry Chemical Physics*, *20*(19), 13153-13158.

Scientific Interests **:** Molecular Biology, Genetics, Biochemistry, Bioinformatics, Polymer Technology, Affinity Techniques